10TH

ANNIVERSARY

HIGHLIGHTS 2016

NÉEL institut

neel.cnrs.fr

EDITORIAL

The Institut NÉEL, Grenoble, was founded ten years ago as a CNRS laboratory devoted to basic research in condensed matter physics, also hosting activities at the interface with chemistry, engineering and biology. Now, as then, a part of the scientific knowledge and technical know-how gained in tackling basic science questions is used for more applied projects, leading in some cases to the creation of start-up companies. Our acquired expertise is also applied to respond to the specific instrumentation needs of other scientific communities (astrophysics, for one) or institutions (the Large Facilities such as ESRF, SOLEIL...), which present new and stimulating challenges.

In line with the strong experimental tradition of our predecessor labs and teams that merged to form the Institut NÉEL, we consider instrumentation both as a key to interdisciplinarity and as a major research axis, along with our condensed matter topics. These topics are, notably: magnetism and spintronics; photonics, plasmonics and non-linear optics; correlated systems, quantum fluids and superconductivity; quantum, molecular and wide-bandgap electronics; and the synthesis, structure and functions of materials. Transverse to all these subjects, theory and its methods provide another key to interdisciplinarity.

The present issue of the Institut NÉEL's annual Highlights magazine contains a sample of our most recent scientific and technical achievements, an article on our outreach to high school students, and a special, illustrated article to mark our 10 years of existence.

Compared to the 500 research papers published in 2016, or to our more than 100 ongoing funded research projects, these specific examples cannot of course do full justice to the wide range of activities present at the Institut NÉEL. However, they do illustrate some of the strong points of our present activity: new magnetic phases, quantum phase transitions, 2D materials and their physics, coherent optics, materials science and superconducting photon detectors... and the long awaited helium liquefier upgrade!

I trust that you will enjoy reading this 2016 issue of our Highlights magazine.

Étienne BUSTARRET

Director of Institut NÉEL, CNRS-UGA

Grenoble, France

The Institut NÉ
maintaining a 50 year-old traditi

The Institut NÉEL was founded as a CNRS research unit in January 2007 by merging four CNRS laboratories located on the Polygon science campus of the Grenoble "Peninsula" : the Centre de Recherche sur les Très Basses Températures (CRTBT), the Laboratoire Louis Néel (LLN), the Laboratoire d'Etude des Propriétés Electroniques des Solides (LEPES) and the Laboratoire de Cristallographie (LdC). These labs were joined by a team from the Laboratoire National des Champs Magnétiques Intenses (LNCMI) and three teams from the Laboratoire de Spectrométrie Physique. The Polygon labs themselves had resulted from the decisions of Louis Néel and Louis Weil to move their historic laboratories from downtown Grenoble to the new CNRS campus in 1962.

Alain Fontaine,
Director
from 2007 to 2010

Alain Schuhl,
Director
from 2011 to 2014

During these first ten years, our research teams and technical services and the Institute's three departments have changed their names and composition, and there has been a sizable but natural turn-over of our permanent staff of around 300 persons. But the strong impetus given to this collective venture by its founders has been maintained. It was significantly strengthened two years ago when our new Nanosciences building was completed, in parallel with the refurbishing of many of the existing labs: experimental results are now being obtained that had previously been out of reach.

We must recognize the efforts made by the Institute to properly address gender equality and safety issues; to contribute to the convergence of the local universities (now become Université Grenoble Alpes and Grenoble-INP); to foster an international atmosphere (over 40 nationalities are represented in our laboratory); and to open the lab regularly to high-school teachers and their students. For all these efforts, and for many other

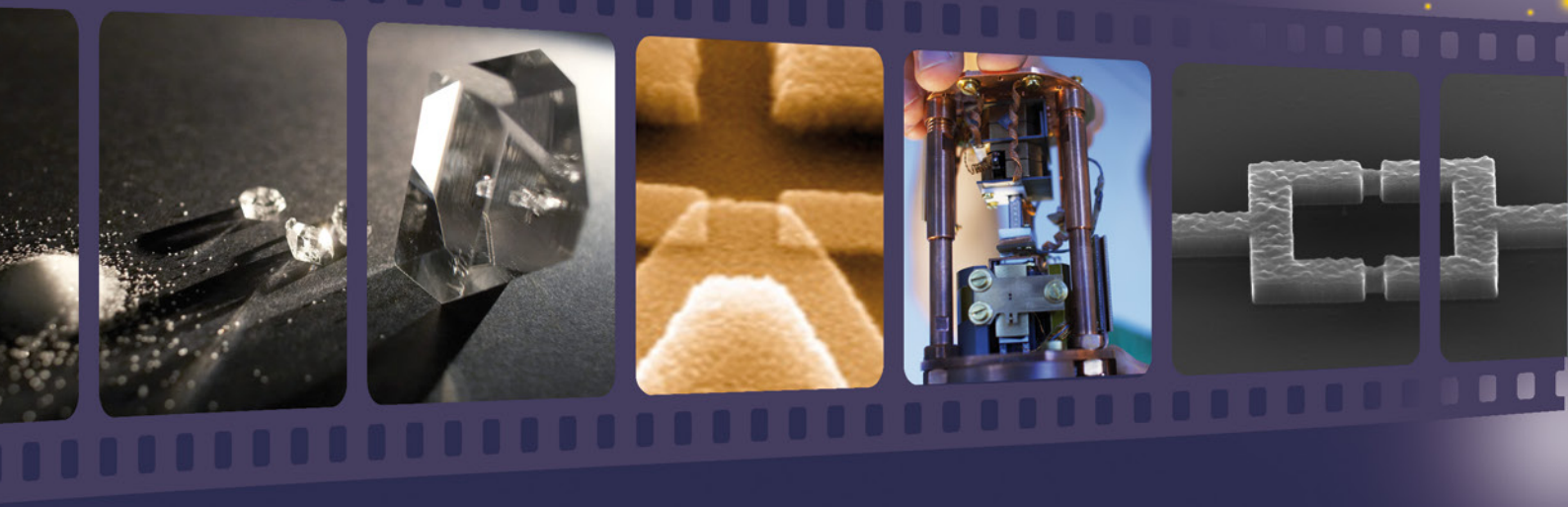

EL at 10 years
on in condensed matter research

Hervé Courtois,
Director
2015

Etienne Bustarret,
Director
2016

accomplishments, we must acknowledge the determining influence of the Institute's first three Directors, Alain Fontaine, Alain Schuhl and Hervé Courtois, as well as the work of their deputy directors, in particular our first technical director, Philippe Gandit.

Ten years ago, "nano" was the main catchword used to promote condensed matter science. It stood for an ambition to probe, measure, manipulate, simulate, and understand individual objects at the nanometre scale. Besides pushing instrumentation, experiment and theory to new limits, these objectives have often brought together chemists, physicists and engineers, and have also led to new knowledge relevant to various other length scales. But of course, our research teams have obtained many important scientific results well outside this "nano" theme over these ten years. At the present time, the word "quantum" might provide a similar additional driving force. We aim again at probing, measuring, manipulating, simulating and understanding; but this now concerns the amplitude and the phase coherence of wavefunctions associated with individual or multiple photons, electrons or other particles, at the low energy end of condensed matter physics. In this context, we are developing additional interfaces with optics and computer science, among other fields.

Whatever the catchword — and whether it be by performing cutting-edge research, or by collaborating actively within and beyond our field of expertise, by training students, by disseminating science to the public, or by valorizing our intellectual property through partnership with industry — our laboratory is keeping up the legacy left to us by Louis Néel.

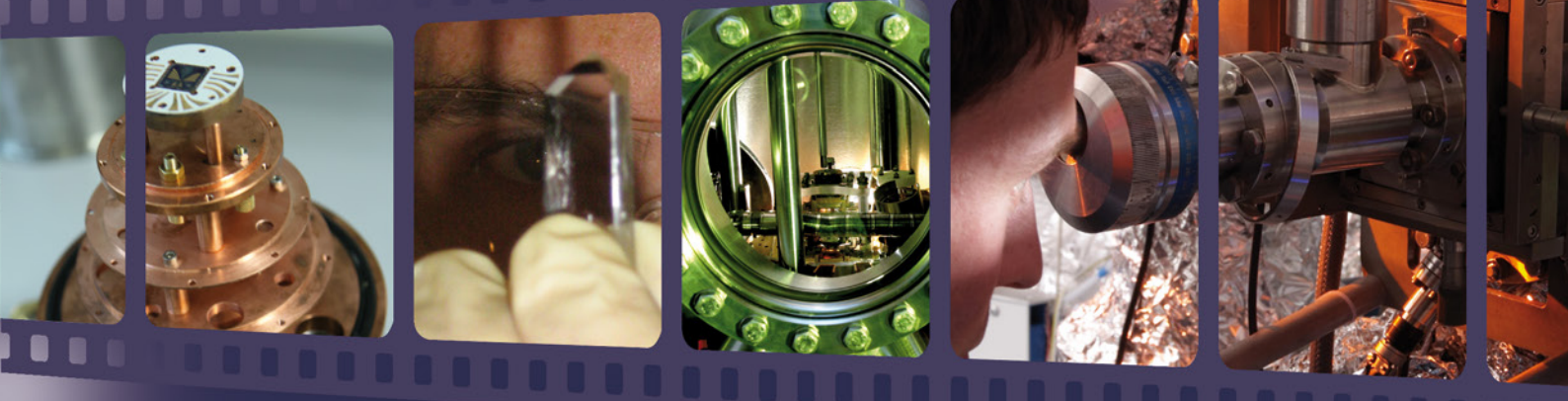

DIRECTOR OF PUBLICATION
Étienne BUSTARRET

EDITORS
Jan VOGEL
Ronald COX

PRODUCTION MANAGER
Nathalie BOURGEAT-LAMI

LAYOUT
Élodie BERNARD
Florence FERNANDEZ

PRINTING
Press'Vercors
December 2016

CONTENTS

Kondo phase shift in quantum point-contacts

A quantum point-contact is a very small constriction in a plane of electrons, defined by gate electrodes. At temperatures near absolute zero, in addition to the well-known quantization of its conductance, this device exhibits anomalous features attributed to strong Coulomb interactions between electrons in the constriction. The nature of this correlated electronic state is not yet understood and novel experiments are needed to get new information, in particular to determine the phase of the electron waves exiting from the constriction. This can be done by using the ultra-sharp tip of a Scanning Gate Microscope to create interference effects in these waves.

In quantum mechanics, electron transport through nanometre-scale devices is characterized by transmission and reflection coefficients which are complex numbers, with real and imaginary parts, meaning that not only the modulus contains information, but also the phase. Though the phase is rarely probed in usual electrical transport experiments, it can sometimes be the unique signature of a physical phenomenon. However, measuring the phase of the transmitted electron waves is not trivial. It requires the realization of an interferometer to convert the scattering phase into a change of the conductance magnitude through an interference effect.

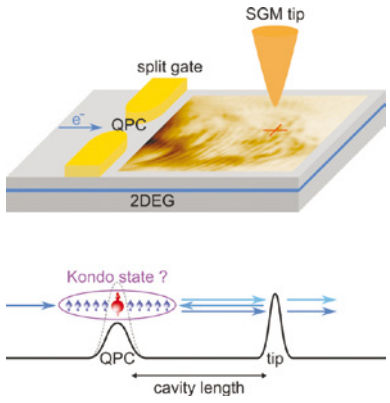

***Fig. 1 (a)**: A metal gate (yellow) with a 300 nm wide split defines a Quantum Point Contact (QPC) between two large reservoirs in a 2-Dimensional Electron Gas (the blue plane) in a GaAs semiconductor device. When a polarized tip (orange) is scanned across the surface, interference fringes appear in a map of the point contact's conductance.*

***(b)**: The tip and the QPC repulsive potentials together form a variable-length, one-dimensional "cavity". The interferences in the cavity are sensitive to the formation of a Kondo cloud of spins around a localized spin situated in the QPC.*

Our quantum point-contact is a 300 nm width x 270 nm length constriction defined in a two-dimensional electron gas by a negatively polarized split-gate electrode (see Fig. 1). This constriction connecting two large electron reservoirs is so narrow that electron waves propagate through it in discrete transverse modes. Each mode can carry current with a quantized conductance of $2e^2/h$. However, this ideal single-particle picture breaks down when the conductance becomes lower than one quantum. An anomalous increase in the non-linear curve of conductance versus the device's source-to-drain bias, the "zero-bias anomaly", appears at very low voltage, see Fig. 2a. In this regime, Coulomb interactions between the very few electrons present in the constriction trigger the formation of a complex many-body state. Its nature is not yet fully understood, but the repulsive interactions are expected to induce localization of one or several electrons within the point contact.

This is propitious for the occurrence of a screening effect first described by Jun Kondo to explain a conductivity anomaly seen in metals containing some magnetic impurity atoms. In our case, electrons of the 2DEG could form a screening "Kondo cloud" of spins around the point-contact, due to their exchange coupling with a localized, unpaired electron spin in the constriction (Fig. 1b). But a clear experimental demonstration of a Kondo effect in quantum point contacts has been missing.

To answer this long-standing question, we did interferometric measurements on a quantum point contact, searching for a particular signature of the Kondo effect, namely its very peculiar phase shift: In the Kondo regime, an electron wave is scattered with a $\pi/2$ phase shift.

We used the ultra-sharp metallic tip of a scanning probe microscope as a local gate to remove all the electrons in a small region of the 2D electron gas at a distance from the constriction (Fig. 1). The electron waves exiting from the quantum point-contact are partly scattered backwards by this depleted region and they interfere with themselves. The resultant change in the device's conductance contains information about the point contact's scattering phase.

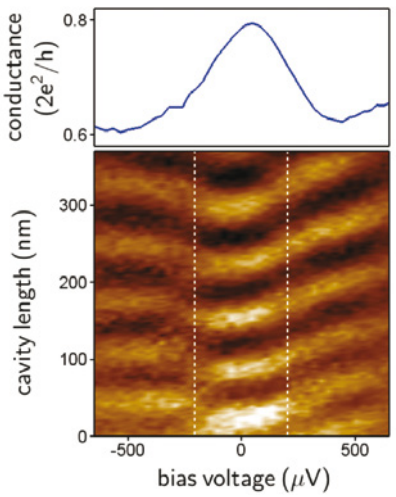

***Fig. 2 (a)**: The zero-bias anomaly at T= 25 mK (an increase in the conductance of the point-contact device as the source-to-drain bias approaches zero).*

***(b)**: The interference fringes, recorded by changing the scanning-tip distance, present a shift in the voltage range (the dotted lines) of the zero-bias anomaly. This shift corresponds to a $\pi/2$ phase shift, consistent with a Kondo effect.*

When we did this experiment at milliKelvin temperature in collaboration with Benoit Hackens at the University Louvain-la-Neuve (Belgium), we observed a clear shift of the interference pattern around zero bias voltage *i.e.* when the ultra-cold electrons travel through the point contact with very small excitation energies (see Fig. 2b). The observed shift corresponds precisely to a $\pi/2$ transmission phase shift, signature of the existence of a Kondo effect for a quantum point contact.

This result confirms the Kondo origin of the QPC zero-bias anomaly, and it illustrates the utility of Scanning Gate Microscopy when other measurements fail to uncover the microscopic origin of quantum phenomena in nanoscale electronic devices.

CONTACT

Hermann SELLIER
hermann.sellier@neel.cnrs.fr

PhD student:
Boris BRUN

FURTHER READING...

"Electron phase shift at the zero-bias anomaly of quantum point contacts"
B. Brun, et al.
***Phys. Rev. Lett.* 116**, 136801 (2016).

"Viewpoint: Kondo physics in a quantum channel"
R. Aguado
***Physics* 9**, 32 (2016).

Complex magnetism in rare-earth iridates

Research in condensed matter magnetism has mainly focused on materials incorporating elements of the 3d transition-metal series (Fe, Co...) and elements of the 4f lanthanide rare earths series (Nd, Tb, Er...). The 3d and the 4f electrons have very different magnetic properties. Both properties can be combined to obtain a great variety of magnetic phases and to make outstanding permanent magnets, like $Nd_2Fe_{14}B$, used industrially in numerous devices. Now, new and fascinating territories are being explored using the 5d transition-metal elements – such as iridium – two rows below the 3d elements in the Mendeleev table.

The 5d electron shell has much more spatial extension than the 3d shell, which at first sight would imply more-delocalized electrons with weaker electronic correlations leading only to trivial paramagnetism. However, the 5d electrons are characterized by much larger spin-orbit interactions that strongly increase with the atomic number Z. It follows that the spin and orbital degrees of freedom are strongly entangled (mixed quantum mechanically), as pictured in Fig. 1. As a matter of fact, the spin-orbit interactions become comparable to the electron-electron correlations and to the crystal-field interactions. Consequently, one can expect unusual metal-insulator transitions, electronic phases with novel topological properties (meaning that they cannot deform continuously into standard electronic phases), or spin-orbit entangled magnetism producing exotic magnetic states and excitations.

We are currently studying a family of oxides with formula $R_2Ir_2O_7$. The iridium ions (Ir) and the rare earth ions (R) form two interpenetrating lattices of the "pyrochlore" type within the crystal. Each of these lattices consists of tetrahedra joined by their corners (*e.g.* Fig. 2a shows the Ir sublattice).

It is known that the pyrochlore iridates $R_2Ir_2O_7$ can undergo an electronic metal-insulator transition, driven by the iridium spin-orbit interaction. This occurs at the same time as the magnetic ordering of the iridium sublattice. Besides, these compounds have been predicted to host a novel type of electronic phase below this transition, called a Weyl semi-metal. An experimentally observable signature of such a phase would be the occurrence of a peculiar "*all-in all-out*" magnetic order of the iridium sublattice at the metal-insulator transition. That is, all the iridium magnetic moments would be pointing either toward or away from the centre of each tetrahedron (Fig. 2a).

Unfortunately, the magnetic order in the iridates is very difficult to probe since the iridium magnetic moment is tiny. To overcome this problem, we have chosen to probe the iridium magnetism via its influence on the magnetic rare-earth. We have thus decided to compare two different rare-earths, Terbium (Tb) and Erbium (Er), which have very different magnetic anisotropy properties: In terbium iridate $Tb_2Ir_2O_7$, the terbium ions' magnetic moments want to align along their local <111> directions (*i.e.* along the diagonal directions joining the corners and the centres of each tetrahedron (Fig. 2)). In $Er_2Ir_2O_7$, the Erbium ion moments want to lie in a plane perpendicular to the <111> directions.

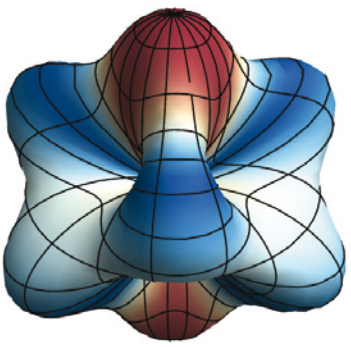

***Fig. 1**: Spin-orbit entanglement in iridates visualized through the iridium's electronic wavefunction. The surface of constant amplitude of electronic probability is shown with the red/blue/white colours corresponding to spin up/spin down/mixed states.*

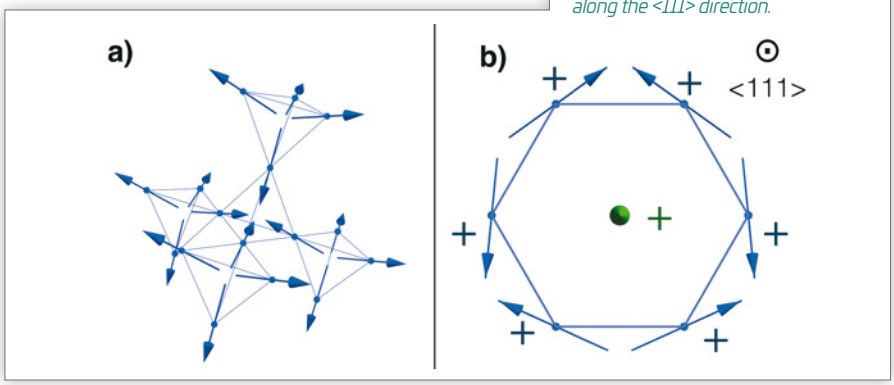

***Fig. 2 (a)**: The "all-in all-out" ordering in the iridium sublattice of $R_2Ir_2O_7$: For any given tetrahedron of iridium ions, all four Ir magnetic moments either point in or point out together along the local <111> directions.*

***(b)** The six Ir nearest-neighbours are situated on a hexagon, surrounding a central Terbium ion. Their magnetic moments, in the all-in all-out configuration, all have a component pointing out of plane (+ direction), thus producing a magnetic field at the Tb site along the <111> direction.*

We have done magnetization measurements and neutron scattering to investigate these two compounds. We find that the Tb sublattice in the terbium iridate develops an *all-in all-out* magnetic order below 40 K. On the other hand, in the erbium compound, the Er sublattice remains disordered down to our lowest measurement temperature of 80 mK.

This contrasting behaviour is explained by the interaction between the iridium and the rare earth magnetic moments. The *all-in all-out* order of the Iridium moments produces a local magnetic field along the <111> directions on each rare earth ion site (Fig. 2). This magnetic field is compatible with the magnetic anisotropy of terbium, the Tb magnetic moment getting aligned along the field in the induced *all-in all-out* configuration (Fig. 2). This indirectly proves the *all-in all-out* order of the iridium in this pyrochlore. On the contrary, the magnetic field produced by the iridiums is competing with the erbium's magnetic anisotropy, thus preventing magnetic ordering of the erbiums. This is again compatible with the *all-in all-out* order of the iridiums.

From this novel approach to the iridium's magnetism, through the induced magnetic behaviour of the rare-earth, our experiments have firmly established the *all-in all-out* order of the iridium sublattice. This special type of order is a necessary condition for the occurrence of exotic electronic transport properties, to be searched for in future work.

CONTACT

Virginie SIMONET
virginie.simonet@neel.cnrs.fr

Rafik BALLOU
Rafik.Ballou@neel.cnrs.fr

PhD student:
Emilie LEFRANÇOIS

FURTHER READING...

"Anisotropy tuned magnetic order in pyrochlore iridates"
E. Lefrançois, V. Simonet, R. Ballou, E. Lhotel , A. Hadj-Azzem, S. Kodjikian, P. Lejay, P. Manuel, D. Khalyavin and L. C. Chapon
***Phys. Rev. Lett.* 114**, 247202 (2015).

Charge-carrier puddles in graphene

What is the spatial extent over which a localized charge perturbs the density of the free charge carriers (electrons or holes) in a two-dimensional electron gas? In graphene – a remarkable 2D material where the charge carriers have zero mass – the capacity to screen background charges depends very strongly on the charge-carrier density. When the carrier density decreases, self-consistent screening theory predicts that the effect of electrostatic inhomogeneities can become very long-range. Scanning Tunnelling Microscopy is a powerful technique for investigating this question.

In vacuum or an insulator, in accordance with Coulomb's law, electrostatic interactions are extremely long range, with no characteristic length scale. Inside a conductor, the free charge-carriers move to screen any inhomogeneities of the potential landscape and Coulomb's law is quenched by an extra, exponential-decay term. This term defines a characteristic screening length, over which electrostatic inhomogeneities are smoothed out.

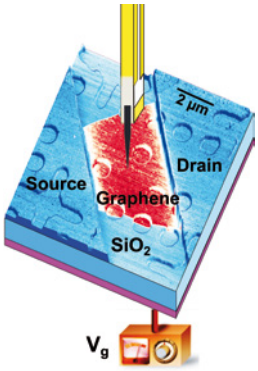

***Fig. 1**: The tip of a Scanning Tunnelling Microscope probes features in the graphene's density of states which contain information about the local concentration of free-carriers, that is, the local electrostatic potential. The graphene's conductance can be probed independently by two lateral metallic contacts (source and drain). The overall carrier density is adjusted by the capacitive coupling to a back gate (V_g) below the graphene.*

Inhomogeneities in the electrostatic environment are of paramount importance for the device performances of 2D electron gases. The electric-potential inhomogeneities are usually caused by nearby, randomly distributed fixed charges, for example in the substrate. The question is then to understand the ability of a conductor to screen variations of the electrostatic background. In conventional 2D electron gases, such as found at the interfaces in semiconducting heterostructures, the ability to screen a fixed charge background does not change with the carrier density. Whatever the concentration of free carriers, the regions of locally lower or higher potential associated with isolated "puddles" (small lakes) of local excess electron or hole density, remain the same in size.

Graphene (a single sheet of carbon atoms) is different. The reason is that, unlike in the usual 2D carrier gases, its charge carriers (both electrons and holes) behave as if they have no mass. Here, it has been predicted that, at the point of vanishing carrier density, the electrostatic screening length should diverge. The carriers form into separated "puddles" whose size diverges and the electrostatics recovers a bare Coulomb-like behaviour. In other words, charge neutral graphene should behave somewhat like an insulator.

To pin down the above prediction experimentally, we have mapped charge-carrier puddles, that is variations of the local electric potential, with sub-nanometre resolution in a graphene device. This was done using a cryogenic Scanning Tunnelling Microscope (STM), see Fig. 1. The main experimental difficulty stems from the fact that the graphene sheet is in a device geometry, meaning that large parts of the substrate (SiO_2) are insulating and thus invisible to the STM technique. This was overcome by combining *in situ* the two rather antagonistic methods of Atomic Force Microscopy (AFM) and STM.

The overall carrier density in the sample of graphene under study is adjusted by applying a potential from a gate electrode situated below the graphene. When and how the graphene is driven to charge neutrality by this gate potential is independently determined by measuring how well the graphene conducts current laterally: when the resistance is maximal, the sample is charge neutral.

The experiment accurately confirmed the above predictions: as graphene goes charge neutral, the potential inhomogeneities grow substantially and in agreement with theory (Fig. 2). Yet, there is a saturation of the size of the inhomogeneities as the carrier density decreases towards zero. This is because, although it may be charge neutral overall, a sheet of graphene is not so at the nanoscale in the presence of a random impurity potential: There are puddles of negatively charged electrons and positively charged holes. A detailed comparison of our experimental results with self-consistent screening theory, done in collaboration with theoretician colleagues of the National University of Singapore, shows very good agreement.

The above-described scenario of the graphene response to charge impurities is implicitly assumed in the prevailing microscopic models, which very successfully describe a large set of electronic transport properties of graphene-based devices. This experiment is the first to check that the underlying assumptions indeed hold, at the microscopic level.

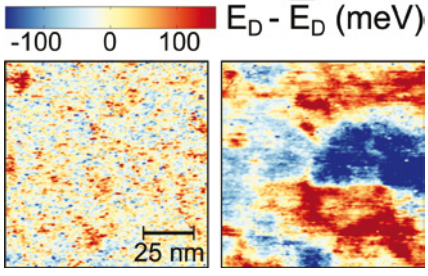

***Fig. 2**: Two maps displaying variations of the local Dirac point energy E_D, that is the local electrostatic potential at different back-gate voltages. At strong hole doping (a), the carrier puddles are short range and of small amplitude. Near global charge neutrality (b), the variations of the potential are very large, both in lateral extent and in amplitude.*

CONTACT

Clemens WINKELMANN
clemens.winkelmann@neel.cnrs.fr

Hervé COURTOIS
herve.courtois@neel.cnrs.fr

FURTHER READING...

"Equal variations of Fermi level and work function in graphene at the nanoscale"
S. Samaddar, J. Coraux, S.C. Martin, B. Grévin, H. Courtois and C.B. Winkelmann
***Nanoscale* 8**, 15162 (2016).

"Charge Puddles in Graphene Near the Dirac Point"
S. Samaddar, I. Yudhistira, S. Adam, H. Courtois and C.B. Winkelmann
***Phys. Rev. Lett.* 116,** 126804 (2016).

"Disorder and screening in decoupled graphene on a metallic substrate"
S.C. Martin *et al.*
***Phys. Rev. B.* 91**, 041406(R) (2015).

Upgrading the Helium Liquefaction Centre

The Helium Liquefaction Centre of Grenoble, situated at the Institut NÉEL, is the largest in France. Each year, about 400 000 litres of liquid helium are distributed to CNRS and university laboratories as well as to the large European research facilities in Grenoble – the European Synchrotron Research Facility (ESRF) and the Institut Laue Langevin (ILL) neutron source. The recent strong demand for more liquid helium has incited us to undertake a major upgrade of our installation and, at the same time, to implement new possibilities for improving its energy performance.

Since 1996, the centre's installation has consisted of two helium liquefiers, both of them using the Air Liquide company's "HELIAL" technology, an adaptation of rotary-screw compressor techniques to the case of helium. The compressor is an essential element in a helium liquefaction installation. Helium gas is cooled by a sequence of compression and expansion cycles. In each cycle, the gas is compressed, which heats it; the heat is extracted via a circulation of oil (which is injected into the gas and cooled in a heat exchanger). An adiabatic and isentropic expansion then cools the gas to a lower temperature.

Our principal liquefier, purchased in 1986, can produce 100 litres/hour and, with various improvements, continues to operate satisfactorily. The second, smaller liquefier has a longer, more complex history- it had been used in the early 1980's in a collaboration with Air Liquide as a test vehicle for their rotary-screw compressor technology. In 1996, a new HELIAL cold box was adapted onto the compressor used in those tests and this liquefier could then produce 60 l/h. It has been used principally as a backup during periods when the bigger Helial is stopped for maintenance or repairs.

In the last ten years, demand has been consistently around 400 000 litres of liquid helium per year. The Helial 100 l/h liquefier can meet the demand but the older liquefier (60 l/h) was becoming inadequate when operating alone as a backup for long periods. Moreover, it was becoming increasingly difficult to maintain its outdated compressor stage, and it had a very high electrical power consumption. The liquefaction facility consumes a total of 2000 MWh of electricity per year. The 60 l/h liquefier consumes 3.6 kW/litre, the 100l/h liquefier only 1.8 kW/litre. There is a potential energy gain here of 475 MWh per year.

Consequently, the liquefaction service undertook a study of ways to upgrade its installations, including an objective of improving the overall energy efficiency. The solution chosen was to replace the older screw compressor, on the 60 l/h liquefier, with a new compressor in order to boost this liquefier's output to more than 100 l/h. In addition, the new compressor would have a frequency variator allowing us to adapt its speed, and thus its energy consumption, to liquid helium production rates.

Though modified somewhat for helium liquefaction, these rotary-screw compressors are actually standard apparatus used in the industrial refrigeration sector. Their constructors can propose a heat exchanger that recuperates the calories generated during the compression phase, in order to heat a building for example. This feature had never been tested on a helium compressor, but the heat produced by the adiabatic compression of helium is potentially very large, because of its high Cp/Cv ratio. We calculated, that for our installation, the energy recuperation potential from this source would be 100 MWh thermal per year. So, it was decided to equip the new compressor with a heat recuperation system.

***Fig. 1**: Arrival of the new helium-gas compressor in the helium liquefaction centre's building at the Institut NÉEL.*

Other improvements to the installation have been made or are in course, such as optimising the working sequences, and installing an energy management system. With these improvements, a 33% overall energy economy (electricity and heating) is predicted.

The upgrade work, started in the autumn of 2015 has been combined with replacement of the automatic control systems and the electrical bays for the two liquefiers, and also a renovation of the rooms containing the helium-recuperation compressors. This work was carried out over 5 months without interrupting liquid helium deliveries and helium gas recuperation.

At present, the new installation is in the trial phase. The upgraded liquefactor is close to attaining its design performance, and the building-heating facility will be tested over the 2016-2017 winter.

CONTACT

Christian GIANESE
christian.gianese@neel.cnrs.fr

FURTHER READING...

Institut NÉEL - Centre de Liquéfaction
http://neel.cnrs.fr/spip.php?rubrique96

High school students discover the world of research

Each year, the Institut NÉEL organizes a series of one-week visits for junior high-school students. Our aim is to give these young students a glimpse of the work that people do in a CNRS laboratory, by introducing them to a selection of subjects from our research programmes.

In France, a week of work experience is required during the "*classe de troisième*", which is the last year of the junior high-school (*collège*). This gives all students 14-15 years old a short introduction to the working world. Our laboratory has been participating in this programme for 10 years now. We provide a concrete introduction to the varied professions exercised at the Institut NÉEL, as well as the courses of study that can lead to them.

Supervised by a small team of tutor-mentors, the young students get direct contact with our personnel. They discover the varied professions represented here: technician, engineer, researcher, information-technology specialist, administrative person, librarian... In small groups and accompanied by staff members, the students learn about these professions, via talks, demonstrations and visits to our research and technical teams. Dialogue is key in this experience.

Over the years our young invitees have been introduced to a great variety of subjects. They are clearly captivated by X-ray diffraction, transmission electron microscopy, cryogenics, liquefaction, crystal growth... Their faces light up with delight when, for example, they see experiments with liquid helium, perfectly colourless and looking just like water, or when they encounter superconductivity via levitating objects!

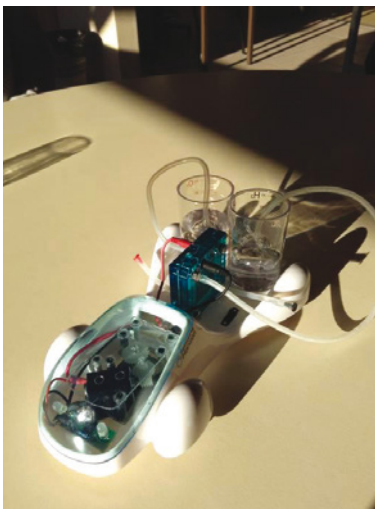

Our young visitors are confronted with complex mechanisms, as for example in this demonstrator fuel-cell.

We take 20 to 30 young students a year, who come to us from different schools and different regions of France, and who are put into groups of five. We have chosen to be totally non-selective in our acceptance policy: students are enrolled on the criterion of "first come, first accepted". This means they have to send their application and cover letter very early, as the sessions fill very quickly each year. We even receive some candidacies already in June for the following school year. In over 90% of cases, the students who come to these sessions at the Institut NÉEL are highly motivated and hard-working, and have a background of good results at school.

An experience around low temperatures.

To provide optimal conditions for these mini-voyages of discovery, we have developed a programme that divides the week into approximately 18 time-slots that last between a minimum of 90 minutes and a maximum of 6 hours (for a short project). This timetable requires the participation of about 15 instructors, with a wide range of expertise. A general call for volunteers goes out each year and the Institute's staff have always been very responsive: We have never found ourselves with the problem of an unfilled time-slot ! Yet the task is not necessarily an easy one, since our participants need to adapt their descriptions and explanations to this quite young audience.

We also provide follow-up and help to the students for the writing of their reports. This is done mostly during the daily luncheon breaks and on their last afternoon, Friday. Also on the Friday our team organizes an afternoon snack that gives our students a final opportunity to do a scientific experiment. They get to try their hand at what we call molecular gastronomy: together, we "cook" an ice-cream cake using liquid nitrogen, and eat it there and then!

The very positive feedback we receive from these students and their teachers encourages us to perpetuate this project. The Institut NÉEL would like to thank once again all the members of staff who year by year involve themselves – with the same enthusiasm – in the smooth running of these "visits of discovery".

CONTACT

Elodie BERNARD
elodie.bernard@neel.cnrs.fr

Grégory GARDE
gregory.garde@neel.cnrs.fr

FURTHER READING...

Further information is available on our website:

http://neel.cnrs.fr/spip.php?rubrique1161

The enigmatic normal state of high temperature superconductors

Superconductivity is a macroscopic quantum state characterized by the total absence of electrical resistance and the ability to fully expel an applied magnetic field. However, these fascinating properties show up only below some characteristic (critical) temperature which, for conventional superconductors, usually does not exceed a few degrees, or a few tens of degrees. So the completely unexpected discovery, in 1986, of new materials where this critical temperature can rise to well above 100 K triggered huge interest. But, despite three decades of intensive studies, understanding the microscopic mechanism at the origin of this unconventional high temperature still remains one of the most challenging issues of solid-state physics.

The main problem is that the fascinating properties of superconductors are also major obstacles to investigation of their physical properties. Indeed, superconductors behave as "black boxes" expelling all electromagnetic probes, hence hindering the investigation of the state that is the immediate precursor to superconductivity. Therefore, it is essential to characterize their non-superconducting state, the so-called "normal" state. But, it appears that the precursor state of the high temperature conductors is far from normal! One of the main ingredients of the standard theory of superconductivity in conventional superconductor systems is the existence of an underlying "good metal" where electrons form a so called "simple" Fermi sea, in which they will be able to form the Cooper pairs that give rise to superconductivity, thanks to their interactions with the lattice vibrations. However, in high temperature superconductors, this calm (Fermi) sea transforms into an extremely rough storm and the nature of the electronic state hiding behind this unconventional superconductivity is still highly debated.

To get access to the precursor normal state it is hence necessary to destroy the superconducting state. This can be done by raising the temperature above the critical temperature (T_c). However, the main difficulty encountered in high temperature superconductors is the presence of several competing magnetic and electronic states. Most of these states are still badly understood (as for instance the mysterious "pseudo-gap" state) and some might yet be discovered. The origin of the high critical temperature is probably ineluctably related to the complexity of their phase diagram, but determining which of these states is essential to the onset of superconductivity or which is, on the contrary detrimental, is an essential – and still extremely debated – step towards our understanding of the mechanism leading to this unconventional superconductivity.

The second way to destroy the superconducting state is to apply a strong magnetic field, while keeping $T < T_c$. Unfortunately in most of the high temperature superconductors the field required to completely destroy superconductivity (called the upper critical field) exceeds 100 Tesla (at zero temperature), much larger than any practically reachable magnetic field. However it has been found recently that, surprisingly, this critical field drops to ~20 T for certain well-defined compositions ("underdoped" non-stoichiometric compositions) of the high-temperature superconductor material YBCO (Yttrium Barium Copper Oxide). This provides the opportunity to destroy the superconducting state in fields available at high magnetic field facilities. The lowering of the upper critical field for this specific material is accompanied by a drastic reconstruction of the electronic structure associated with the formation of an unexpected charge-ordered phase (the electron density becomes inhomogeneous, but with a spatial ordering).

Several probes have been used to investigate the nature of this new charge-ordered state but the most efficient technique to study phase transitions is probably the specific heat (C_p). Indeed, this thermodynamic quantity is directly related to the temperature derivative of the entropy and is expected to present a clear anomaly at any phase transition.

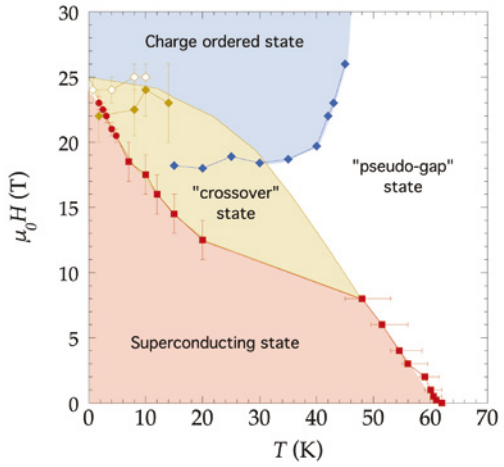

***Fig. 1**: The Magnetic field - Temperature (H-T) phase diagram of underdoped $YBa_2Cu_3O_{6.54}$ single crystals deduced from our specific heat measurements (red symbols) as compared to characteristic phase boundary lines deduced from other experimental probes, namely thermal conductivity (brown symbols) and sound velocity measurements (blue symbols).*

There is clearly an inflection in the specific heat line around 30-40 K highlighting the existence of a broad "crossover" state arising from the competition between the superconducting and the charge-ordered states.

We have developed a high-sensitivity modulation technique that enabled us to study the calorimetric properties of very small single crystals. Specific heat measurements were performed at up to 36T and down to 1.5K at the French National High Magnetic Field Laboratory, Grenoble. A well-defined anomaly could be identified in both the magnetic field and the temperature dependence of C_p. This anomaly (the field where the specific heat deviates from its standard dependence in the superconducting state) is plotted in Fig. 1 (red points). As is seen, the corresponding boundary line in the H-T phase diagram differs strongly from those deduced from other experimental probes such as thermal conductivity (brown symbols) and sound velocity measurements (blue symbols).

Below 20 K, our boundary line has also clearly deviated from the standard upper critical field (the line between the brown and blue regions in Fig. 1 which would mark the onset of superconductivity in a conventional superconductor.

This highlights the presence of a large "crossover" state separating the superconducting state and a charge-ordered, normal state in this material. It most probably originates from the competition between these two states. Our future research will be directed to understanding the significance of this newly discovered crossover-state, in view of solving the enigma of the normal state of high temperature superconductors.

CONTACT

Thierry KLEIN
thierry.klein@neel.cnrs.fr

PhD student:
Bastien MICHON

FURTHER READING...

"Calorimetric determination of the magnetic phase diagram of underdoped ortho II $YBa_2Cu_3O_{6.54}$ single crystals"

C. Marcenat, A. Demuer, K. Beauvois, B. Michon, A. Grockowiak, R. Liang, W. Hardy, D.A. Bonn and T. Klein

***Nature Commun.* 6**, 7927 (2015).

Chromium: a spin qubit with large spin to strain coupling

Quantum two level systems ("qubits") strongly coupled to mechanical resonators can function as hybrid quantum systems with several potential applications in quantum information science. Access to a strong coupling regime, where non-classical states of a mechanical resonator are generated, could be achieved with solid state quantum bits whose energy levels have a large strain response. Thanks to their long coherence time, localized spins of individual magnetic atoms incorporated in a semiconductor host have great potential for storing quantum information in the solid state. The variety of magnetic transition elements that can be incorporated in semiconductors gives a large choice of electronic and nuclear spins as well as orbital momentum. Among these magnetic atoms, chromium is of particular interest, since strain can be used to control its magnetic anisotropy and thus influence its spin state.

Chromium (Cr) is incorporated in Group II-Group VI semiconducting compounds as Cr^{2+} ions carrying a localized electronic spin $S = 2$ and an orbital momentum $L = 2$. Moreover, most of the Cr isotopes have no nuclear spin which simplifies the spin level structure and its coherent dynamics. In the presence of bi-axial strain, the ground state of a Cr^{2+} ion is an orbital singlet with spin degeneracy $2S+1= 5$. The chromium's orbitals are sensitive to modification of the crystal field and thus connect its spin S to the local strain environment via the spin-orbit coupling.

For such a magnetic atom, static strain can be used to control its magnetic anisotropy and thus influence its spin memory. This large coupling of spin to strain, at least two orders of magnitude larger than for magnetic elements without orbital momentum, makes chromium a very promising spin qubit for the realization of hybrid spin-mechanical systems in which the motion of a microscopic mechanical oscillator would be coherently coupled to the spin state of a single atom.

To optically control the spin of an individual atom, we insert it in a quantum dot. In our experiments, the quantum dot is an island of the semiconducting compound Cadmium Telluride CdTe inside a layer of Zinc Telluride ZnTe. Absorption of an incident photon creates an electron-hole pair (an "exciton") in the quantum dot (see Fig. 1). Inversely, a photon is emitted when the electron and hole annihilate each other. With a single Cr atom introduced in the dot, the energy and polarization of the photon emitted or absorbed by the dot depends on the spin state of the magnetic atom (Fig. 1). This is due to the exchange interaction present in the excited state, between the spin of the confined exciton and the spin (S_z) of the chromium.

In our work, we have demonstrated that the chromium spin can be used as an optically addressable qubit. First, the evolution of the quantum dot's optical emission with magnetic field (see Fig. 1) revealed the large sensitivity of the Cr spin to local strain. Next, we used resonant optical excitation of the quantum dot to control and read out the Cr atom's spin state. That is, we have shown that excitation with a laser beam tuned to the wavelength of one of these optical transitions can be used to initialize the state of the Cr spin and to probe its dynamics optically: The Cr atom behaves like an optically addressable, long-lived, spin-based memory.

Under optical excitation exactly resonant with an absorption transition, we can also enter the "strong coupling" regime where hybrid states of matter and light are created. The ground state of the magnetic atom is then "dressed" with light. The spin-dependent strong coupling with the laser field modifies the Cr atom's energy levels. The optically controlled energy shift affects the spin dynamics of the atom and will be used for a coherent optical manipulation of the spin of an individual Cr atom.

Future applications of this new spin qubit in hybrid nano-mechanical systems will exploit the efficient mixing of the Cr spin states S_z= +1 and S_z = -1 induced by anisotropic, in-plane strain (see Fig. 1). The resulting mixed spin states, together with an exciton, form an optical "three level Λ (Lambda) system" (two ground states coupled optically with one excited state). This level structure opens the possibility of using coherent optical spectroscopy techniques for a sensitive probing of the local strain at the atom location and it makes Cr a very promising atomic scale strain-sensor.

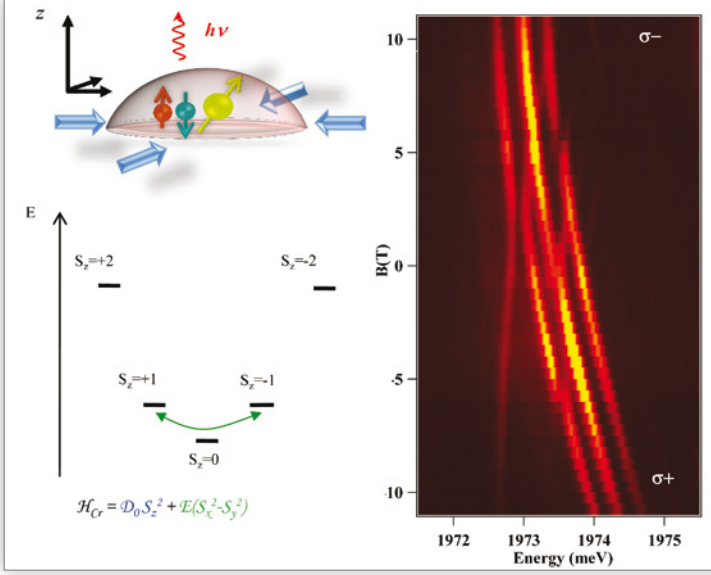

***Fig. 1 - At top**: A strained quantum dot containing a chromium atom (green) and an optically-created exciton (electron and hole, blue and red, with their spins).*

***At bottom**: The energy levels of a Cr spin in the ground state of a quantum dot having large biaxial strain.* The Cr fine structure is dominated by the magnetic anisotropy $D_0 S_z^2$. Anisotropic in-plane strain ($E(S_x^2 - S_y^2)$) couples its spin states S_z= +1 and S_z= -1.

***At right**: The dependence on magnetic field (Bz) of the photoluminescence spectrum (at low temperature, T = 5 K) for a CdTe/ZnTe quantum dot containing a single Cr atom. Only the Cr magnetic ground states Sz= 0 and Sz= ±1 are observed.*

CONTACT

Lucien BESOMBES
lucien.besombes@neel.cnrs.fr

Hervé BOUKARI
herve.boukari@neel.cnrs.fr

PhD student:
Alban LAFUENTE-SAMPIETRO

FURTHER READING...

"Individual Cr atom in a semi-conductor quantum dot: Optical addressability and spin-strain coupling"
A. Lafuente-Sampietro, H. Utsumi, H. Boukari, S. Kuroda and L. Besombes
***Phys. Rev. B* 93**, 161301(R) (2016).

"Strain-induced coherent dynamics of coupled carriers and Mn spins in a quantum dot"
A. Lafuente-Sampietro, H. Boukari and L. Besombes
***Phys. Rev. B* 92**, 081305(R) (2015).

Quantum fragmentation and classical restoration of spins

Consider a small ferromagnetic particle — so small that it contains just a single magnetic domain — placed in a magnetic field. If one reverses the direction of the magnetic field, how fast and via what path does the magnetisation change direction? This problem of classical physics was treated in 1948 by E. Stoner and E. Wohlfarth. Their model, which calculates the (zero-Kelvin) free energy of the particle, has been applied to ensembles of small magnetic particles in many areas of physics, chemistry or metallurgy such as magnetic metal alloys and glasses, mineral solid solutions, steels, gels, ceramics, and the tiny bits on computer hard-disks... More recently, similar models have been developed for nanoparticles and single-molecule magnets, objects so small that their magnetic energy is quantized into discrete values. Here we discuss a fundamental question: Can one link these two very different views of the magnetism of small particles, *i.e.* the classical and quantum physics ones?

Imagine a ferromagnetic nano-scale object, at zero K, with some tens or hundreds of spins coupled to make a large total spin S with a preferential orientation (its anisotropy axis Oz). The spin S, projected on this axis, has $2S+1$ sub-states, M_z. We have investigated, numerically, a theoretical model that has a parabolic energy barrier against spin reversal, a fixed perpendicular field H_x and a sweeping longitudinal field H_z. Fig. 1 shows one example, the 41 energy levels of a spin $S=20$. We have fixed $H_x=1$ and H_z sweeps from +1 at the right of the Figure to -1 at the left, at a constant rate c. The resultant field rotates from +45° to -45°. (Our Hamiltonian is, in reduced units, $H=-Ds_z^2-H_x s_x-H_z(t).s_z$, with the anisotropy parameter $D=1$ and with reduced spins $s_x=S_x/S$, $s_y=S_y/S$, $s_z=S_z/S$ to catch the proper limit as S approaches infinity.)

Starting from large positive H_z at the right of Fig. 1, the ground-state $M_z=20$, well separated from the higher levels with $M_z=19, 18$ ..., is essentially not mixed (it is quasi-classical) and, since $T=0$ K, its probability of occupation is 100%. This ground state remains fully occupied until $H_z=0$ where the first level-crossing between S and $-S$ is reached. Because of the perturbative effect of H_x, this is an avoided level crossing (an "anticrossing") so the system can, in principle, switch from $M_z=+20$ to $M_z=-20$, but the probability of this is vanishingly small for these large M_z states, even at very low sweeping rates.

For $H_z<0$ (at the left in Fig. 1), the state $M_z=S=20$ is no longer the ground state. We now call it the metastable state — or metastable branch. As the field-sweep continues, this state crosses the levels $M_z=-19$, ..., $-S+k$, ... The exponential increase of the successive anti-crossing gaps (which are proportional to $(H_x/DS)^{2S-k}$) makes spin-reversals and spin-mixtures more and more probable until the semi-classical spin S scatters along the different states below the metastable branch. We now call this spin "fragmented".

In collaboration with colleagues in Japan, we have calculated, numerically, the Quantum Dynamics of such a system at zero Kelvin with S ranging from 20 up to 320. More particularly, we have calculated for each spin value the integrated probability of spin-reversals associated with full field-sweeps, going from large positive to large negative fields H_z. We showed that all the data can be merged on to a single scaled dynamical curve as a function of S and $H-H_{SW}$ (Fig. 3 of Hatomura *et al.* 2016). Interestingly, this scaling curve valid for large quantum spins up to infinite (*i.e.* classical) spin shows that quantum dynamics is permitted for any field H_z between zero and H_{SW}. However, as expected, the probability of spin reversal goes to strictly zero there as S approaches infinity, except at the threshold $H=H_{SW}$ where spin reversal onsets very sharply in these calculations, as in the classical-physics model.

Furthermore, this function turns out to be identical to the scaling curve of the so-called "Spinodal" Phase Transition, a very general process in physics, where this function represents the probability to find "non-yet-flipped" particles in an ensemble of N diffusing particles subjected to external (usually thermal) fluctuations. This suggests that a large quantum spin S could be regarded as an ensemble of N = $2S$ spins ½ (↑ and ↓) having the possibility of one or more spins flipping from ↑ to ↓ at the different anti-crossings of the metastable branch. The integrated probability of spin-reversals near and at the Stoner-Wohlfarth reversal field H_{SW} (the red vertical bar in Fig. 1), our spinodal phase transition, can then simply be associated with the "fragmented" spin resulting from the spin-flips at the successive $S\rightarrow -S+k$ anti-crossings (k spin-flips).

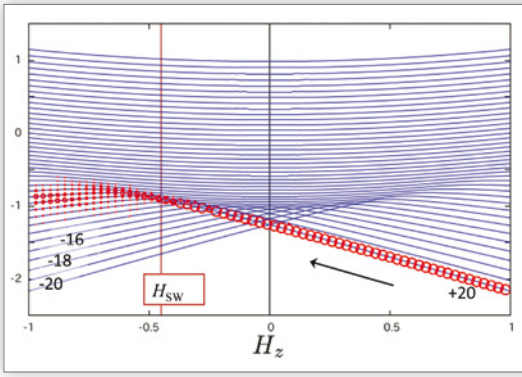

***Fig. 1**: Energy spectrum for a spin S=20. The longitudinal field H_z sweeps from right to left, which leads to spin-reversals from the ascending energy level (m =+20) to the descending levels when H_z is negative and large enough. The gaps at each avoided level crossing cannot be seen at the scale of the Figure. The sizes of the red circles indicate the probabilities of occupation of the states at zero Kelvin.*

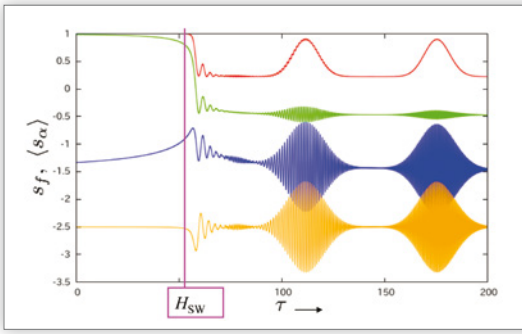

***Fig. 2**: As the field sweep continues (from left to right at constant rate c) beyond the Stoner-Wohlfarth transition at H_{SW}, the calculations yield temporal beats of (from bottom to top) the expectation values of S_x, S_y, S_z, and the spin length. This beating represents the long-range spinodal modulations of the Stoner-Wohlfarth model.*

Since a consequence of the spinodal phase transition is an onset of a modulation of the order parameter, one should expect the emergence of a stable sinusoidal modulation of the spin dynamics as a function of H_z (and so with time) as H_z is swept (at constant rate c) more negative than H_{SW}. This is precisely what we found (in the absence of damping/decoherence): The calculations show long-period modulations of the "restored", *i.e.* no longer "fragmented" precession of the whole spin S, see Fig. 2. Constituting a new characteristic of Quantum Dynamics, these spin beats can also be viewed as resulting from classical interferences of the superposed spin-states ($M=-S, -S+1, -S+2, ..., S$).

Experiments are planned to observe the spinodal dynamical scaling, and also the spin beating (though this would be harder). Among the numerous outlooks of this study, the most obvious one is achieving better understanding of the nature of the quantum to classical transition.

CONTACT

Bernard BARBARA
bernard.barbara@neel.cnrs.fr

FURTHER READING...

"Quantum Stoner Wohlfarth Model"
H. Hatomura, B. Barbara and S. Miyashita
***Phys. Rev. Lett.* 116**, 037203 (2016).

"Mesoscopic systems: classical irreversibility and quantum coherence"
B. Barbara
***Phil. Trans. R. Soc. A* 370**, 4487 (2012).

Probing the anisotropy of optical fibres by Third Harmonic Generation

An optical fibre is a fantastic tool for confining light over a huge distance, especially in modern telecommunications. We now have available a broad range of optical fibres for diverse uses. For most applications, any effect that modifies the polarization of the light propagating in the fibre must be avoided. How can we accurately characterize these parasitic polarization effects, which are linked to unwanted birefringence in the fibre? It can be done using a protocol of nonlinear crystal optics, specifically Third Harmonic Generation experiments.

Third Harmonic Generation (THG) is a nonlinear interaction based on the third-order electric susceptibility of matter. It can exist in any medium, *i.e.* gas, liquids, glasses, crystals, without any restriction of symmetry. From the quantum point of view, it corresponds to the collapse of three photons into one, as shown in Fig. 1. So if $h\nu$ is the quantum of energy of each incident photon, where ν is the frequency of the associated wave, then the quantum of energy of the photons produced by third harmonic generation will be $3h\nu$, the corresponding wave being the third harmonic of the incident wave, which is then called the fundamental wave.

An optical fibre is a dielectric waveguide that confines the electromagnetic field in a cylindrical geometry. For the light to propagate, the fibre takes advantage of the physical phenomenon of total internal reflection, as shown in Fig. 2. In a collaboration with the cable company DRAKA, we have studied a 642-mm-long fibre of their design. This optical waveguide is made of two concentric cylinders of isotropic glasses (Fig. 2): The inner one is the core, made of silica (amorphous SiO_2) doped with a molar concentration of 37% of Germanium dioxide (GeO_2) of radius a = 2.19 µm, and the outer one is the "cladding", of larger radius and made of undoped silica. The light is confined in the core since its refractive index is much higher than that of the cladding.

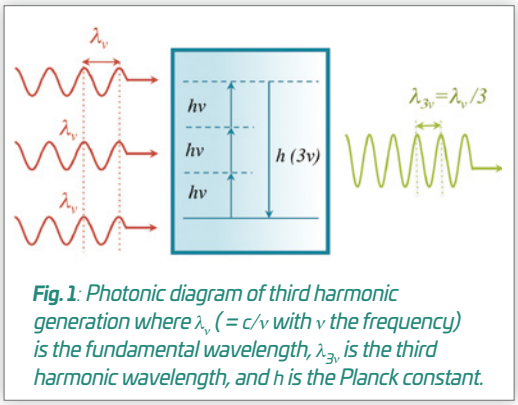

***Fig. 1**: Photonic diagram of third harmonic generation where λ_ν (= c/ν with ν the frequency) is the fundamental wavelength, $\lambda_{3\nu}$ is the third harmonic wavelength, and h is the Planck constant.*

This fibre should be fully isotropic. That is, the refractive index should keep a fixed value whatever the direction of polarization of the light. By studying third harmonic generation in this fibre, we have demonstrated that in fact it exhibits a significant anisotropy of the refractive index as well as of the third order electric-susceptibility tensor.

Contrary to the case of crystals exhibiting birefringence, *i.e.* crystals having, for a given direction of propagation, two possible values of the refractive index according to the polarization of the light, the only way to perform third harmonic generation efficiently in an optical fibre is to exploit two different modes of propagation for the two waves at ν and 3ν. These two modes will necessarily exhibit different geometries, but there may exist a frequency ν for which the effective refractive indices of the fundamental and third harmonic waves are equal, leading to momentum conservation and thus to a maximization of the THG efficiency. In the case of the fibre we used, this situation can be achieved when the fundamental wave is in the linearly polarized (LP) mode called LP01 at an expected value of λ_ν = 1550 nm, and the third harmonic wave, *i.e.* at $\lambda_{3\nu} = \lambda_\nu/3$, is in the LP03 mode, as shown in Fig. 2.

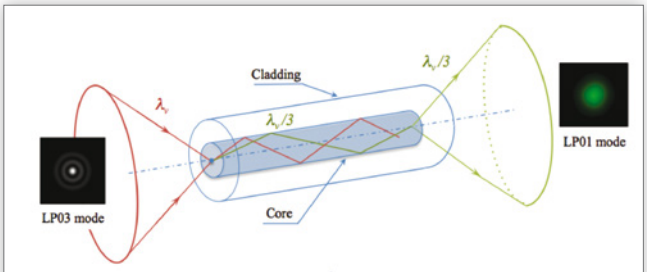

***Fig. 2**: Third Harmonic Generation performed in a step-index optical fibre. The two images show the transverse intensity profiles of the fundamental wave in the fibre's LP01 mode and of the third harmonic wave in the LP03 mode.*

We measured the spectrum of this third harmonic wave for different orientations of the linearly polarized fundamental wave. We found that the wavelength where third harmonic generation is observed, *i.e.* $\lambda_{3\nu}$, varies between two extreme values, *i.e.* 516.4 nm and 516.9 nm, corresponding to two particular perpendicular directions of polarisation. This difference of wavelength indicates that the refractive index of the fibre is anisotropic, and it can be used to estimate the birefringence, which we found to be equal to 9×10^{-5}.

From measurements of the intensity of the third harmonic wave as a function of the polarization angle of the fundamental wave, we observed a complex polarization behaviour. Since this fibre is not coiled, that is to say it is without any extrinsic mechanical stress, we explain the results by stating that the fibre exhibits an intrinsic uniaxial strain due to the material itself. We performed calculations by taking into account the non-linearity under strain and all the possible configurations of polarization for the fundamental and third harmonic waves and we found a remarkable agreement between measurements and calculations.

Thus, we have demonstrated that Third Harmonic Generation provides an excellent tool for analyzing the weak intrinsic anisotropy of an optical fibre. Also, this work should allow us to best design a method, using fibres, for the generation of "triple photons", a new state of light produced by third order spontaneous parametric down-conversion, which is the exact reverse process of third harmonic generation.

CONTACT

Benoît BOULANGER
benoit.boulanger@neel.cnrs.fr

Corinne FÉLIX
corinne.felix@neel.cnrs.fr

PhD student:
Adrien BORNE

FURTHER READING...

"Multiple intermodal phase-matched third-harmonic generations in a silica optical fiber"
A. Borne, T. Katsura, C. Félix, B. Doppagne, P. Segonds, K. Bencheikh, J.A. Levenson and B. Boulanger
***Optics Communications* 358**, 160 (2016).

"Anisotropy analysis of third-harmonic generation in a germanium-doped silica optical fiber"
A. Borne, *et al.*
***Optics Letters* 40**, 982 (2015).

Theory for organic systems: the Fiesta initiative

Nowadays, the development of efficient computer codes that exploit the basic principles of quantum mechanics for the study of condensed-matter systems requires a merging of expertise between physicists, applied mathematicians and computer scientists. Collaborative work of this kind, between the Institut NÉEL and the Institute for Nanosciences and Cryogenics (INAC), has created a source code named FIESTA ("French Initiative for the Electronic Structure of Thousands of Atoms"). This code is being used to study organic systems of interest for electronics, photovoltaics, light-emission, wet chemistry and biology. The collaborating teams received the national 2014 Bull-Fourier prize for the use of computer sciences in physics.

Theoretical studies of the electronic properties of condensed matter systems rely on the basic rules of quantum mechanics. Even though these have been known since the early 20th century, the very large number of degrees of freedom (there are typically 10^{23} electrons per cm^3 of matter) precludes an exact, direct solution of the relevant equations that would yield the information needed to characterize the system of interest. It is the art of the theoretician to simplify the basic equations, and/or to reduce the number of degrees of freedom, in a way that preserves the accuracy needed for the properties or the experiment we want to describe.

A powerful approach to rationalizing how to classify the electron-electron interactions within a system by order of importance is called "many-body perturbation theory" (MBPT). This approach allows us to understand how to tune the needed accuracy by incorporating important effects before fine corrections. Such methods are built so that the first electron-electron interactions to be considered capture the most important effects while being computationally the most reasonable. This is clearly a crucial result which relies on several decades of theoretical studies.

While developed at the "pen and paper" level in the 1960s, a second step is the efficient implementation of these theories in the available computers, a crucial aspect that requires not only an expertise in physics, but also in applied mathematics, computer languages and computer architectures. Such a merging of expertise was initiated in 2011 between the Institut NÉEL and the Simulation Lab (*Laboratoire de Simulation Atomistique L_Sim*) at INAC, Grenoble. The aim was to develop a modern modelling tool, called the "Fiesta" code, devoted to studies of organic systems of interest in electronics, light-harvesting, light-emitting devices, wet chemistry and biology.

The specific many-body perturbation theory techniques implemented in the Fiesta code originate from the solid-state physics community. These methods rely on the concept of "screening" in semiconductors and metals, namely the fact that in a solid the effective interaction between two electrons is "attenuated" by the other electrons. What the Fiesta team have demonstrated is that such techniques can also be very efficient in the description of organic systems where such screening phenomena are much weaker. This leads to the description of the electronic and optical properties of a very large class of organic systems (small molecules, polymers, isolated or dense phases, etc.) to remarkable accuracy with limited computing-time cost. In particular, we have used the Fiesta code to explore the basic mechanisms behind the conversion of light energy into an electric current in organic photovoltaics (Fig. 1), and to understand how doping works in organic semiconductors. This has allowed us to discriminate between the several scenarios proposed for these phenomena.

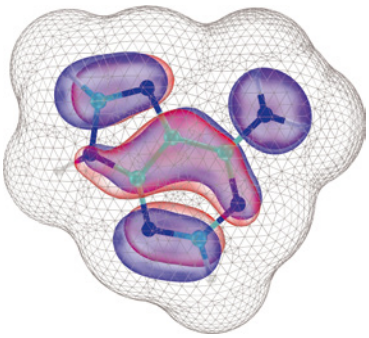

***Fig. 2**: Symbolic representation of an adenine molecule (one of the four DNA bases) placed in an effective water solvent. Here, FIESTA has described the biologically important interactions of the adenine molecule with H_2O molecules (screening, polarization, dipolar interactions, etc.) by induced effective charges on the solvation shell represented as a mesh. The colour shows the shape of the adenine's highest occupied electronic orbital (Duchemin, Jacquemin & Blase, 2016).*

Ongoing projects concern the merging of these many-body perturbation theory techniques with less-sophisticated techniques that are less accurate but more efficient in computer-time. These techniques can describe the effect of a medium (other molecules, an inorganic substrate, an electrode, etc.) that surrounds the molecule or "active subsystem" that is being described with the best MBPT methods (Fig. 2).

This is the sort of mix of quantum mechanical and semi-classical techniques that was recognized by the 2013 Nobel prize in Chemistry. Such techniques are essential steps for bridging the gap between present computer simulations and precise descriptions of a large class of systems of interest in physics, chemistry, and biology.

***Fig. 1**: Symbolic representation of the theory-to-application flow. **At left:** Many-body perturbation theory (Feynman diagrams). **Centre:** Your best computer. **At Right:** Dissociation of a photoelectron-photohole pair at a model donor-acceptor interface with proper, screened, electron-hole interactions.*

CONTACT

Xavier BLASE
xavier.blase@neel.cnrs.fr

PhD student:
Carina FABER

FURTHER READING...

Review article:
"Excited states properties of organic molecules: from density functional theory to the GW and Bethe-Salpeter Green's function formalisms"

C. Faber, P. Boulanger, C. Attaccalite, I. Duchemin and X. Blase

***Phil. Trans. R. Soc. A.* 372**, 20130271 (2014).

Revealing coherence of single emitters with photonic nanostructures

Physicists usually associate coherence with macroscopic interference patterns, as observed for example in the famous experiment where light waves are passed through a double-slit. Astonishingly, interference is also generated when photons are launched one-by-one, as if they were capable of going through both slits at the same time. This can only be explained by acknowledging that individual photons go through a double-slit in a quantum superposition state. Such states, carrying microscopic coherence – that seem so bizarre and hidden to our "common sense" – are ubiquitous in the quantum realm. The example of the laser, which exploits macroscopic coherence, indicates that it would be not only exciting, but also useful to harness microscopic coherence. So how can we reveal it?

Accessing and manipulating coherence of single quantum objects – like photons, atoms, molecules, or emitters embedded in solids – is at the forefront of physics, especially at the intersection of quantum optics, condensed matter and information processing. The key to accomplish such advanced tasks is to conceive a robust interface between our clumsy detection apparatus and the object studied.

Take, for example, emitters in a solid. One can produce these at low temperature by shining light on a semiconductor and exciting a cloud of electrons and holes attracting each other. We have learnt over the last two decades to trap and isolate a single electron-hole pair within a nanoscale "Quantum Dot" (QD) inside the semiconductor. As the trapped electron-hole pair possesses a dipole moment, it strongly interacts with light and annihilates, sending out a photon approximately every nano-second. A great deal of research has been devoted to study such emission, now resulting in innovative commercial products such as quantum dot displays. Rather more at the development stage, quantum dots are becoming a leading resource for high repetition rate, single photons – a crucial asset in future quantum technologies that will exploit entanglement and indistinguishability of photons.

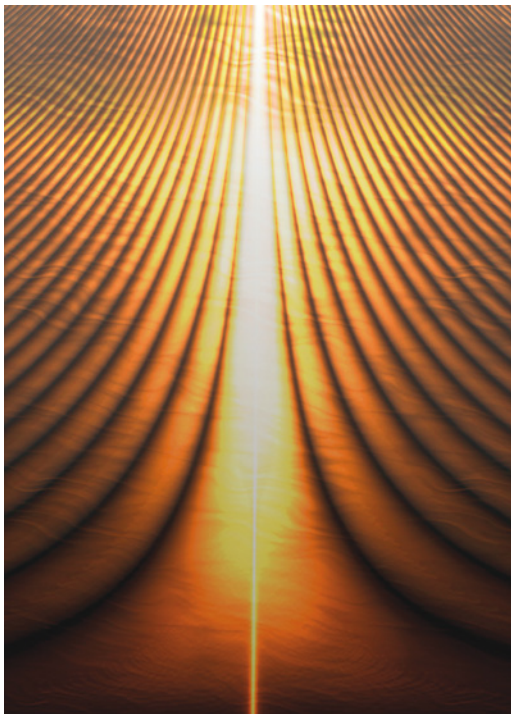

***Fig. 1**: Graphical representation of our multi-wave, coherent-manipulation scheme, as applied to an individual exciton (an electron-hole pair) confined in an Indium Arsenide quantum dot. In this colour-coded map, the horizontal axis displays the four-wave mixing spectrum of a single quantum dot. The vertical axis is the delay between a control pulse and the four-wave mixing signal. The control pulse stops the four-wave mixing transient, inducing shaping of the four-wave mixing spectrum. (Figure credit: Florence Fernandez, Institut NÉEL.)*

While observing the emission from a quantum dot has become an easy task, detecting the dot's absorption – which holds information about the coherence of the resident quantum dipole – is arduous. In our experiment, we use 100 femto-second (10^{-13} sec) laser pulses, centred at the wavelength of the expected optical absorption (which is around 1000 nanometres for our Indium Arsenide/Gallium Arsenide QDs). The pulses are so short that the uncertainty principle intervenes and they undergo spectral broadening by several nanometres. Thus, the pulses constitute an equivalent "white light" source for measurements of the quantum dot's picometre (10^{-12} m) wide absorption band. Using a microscope we focus the laser beams onto the quantum dot and observe the spectrum of the reflected light, where we look for an absorption dip.

The huge difficulty in this experiment is that the "white light" laser intensity dominates the dot's response by typically 12-15 orders of magnitude – it is as if one were trying to observe sunspots by gazing at the sun with a naked eye (which is strongly discouraged!).

Rejection of this overwhelming background is the key aspect of our technique. It is accomplished in a three-fold manner. Firstly, instead of one we use three laser pulse trains and modulate their relative phases. Thus, the resulting third-order absorption – called four-wave mixing – within the QD is also modulated, and we simply demodulate it as in an old-fashioned radio. Secondly, the signal is detected via interfering it with yet another laser beam, improving the detection sensitivity.

Finally, specially for this project, which involved eight French and European teams, our colleagues have conceived novel "nanophotonic" structures with embedded quantum dots, specifically semiconductor microcavities, photonic-waveguide antennas and microlenses. With these devices we can amplify the electromagnetic field locally around the dot to penetrate efficiently across the vacuum-dielectric boundary. This drastically decreases the "white light" background and improves the signal-collection efficiency, increasing the sensitivity for retrieving the single emitter coherence by four orders of magnitude.

This experiment then provides unprecedented insight into the dynamics and the control of the optical coherence of single emitters in solids. In ongoing research, we have introduced a spatial separation between the three beams. The beams now selectively excite a pair of emitters embedded in a photonic waveguide, to induce their non-local coupling, mediated by the microscopic coherence.

CONTACT

Jacek KASPRZAK
jacek.kasprzak@neel.cnrs.fr

PhD students:
Quentin MERMILLOD
Valentin DELMONTE

FURTHER READING...

"Harvesting, coupling and control of single exciton coherences in photonic waveguide antennas"
Q. Mermillod, T. Jakubczyk, V. Delmonte, A. Delga, E. Peinke, J.-M. Gérard, J. Claudon and J. Kasprzak
***Physical Review Letters* 116**, 163903 (2016).

"Multi-Wave Coherent Control of a Solid State Single Emitter"
F. Fras, Q. Mermillod, G. Nogues, C. Hoarau, C. Schneider, M. Kamp, S. Höfling, W. Langbein and J. Kasprzak
***Nature Photonics* 10**, 155 (2016).

"Dynamics of excitons in individual InAs quantum dots revealed in four-wave mixing spectroscopy"
Q. Mermillod, *et al.*
***Optica* 3**, 377 (2016).

New multiferroics inspired by minerals

Multiferroics are materials that show both magnetism and ferroelectricity (spontaneous electric polarization) at the same time. A coupling of electric fields and magnetic fields in materials was speculated as early as 1894 by Pierre Curie. However, magnetism and ferroelectricity are generally antagonistic properties and multiferroics have long remained rather rare "creatures". Recently, it has been understood that some specific types of magnetic order can induce ferroelectricity, and this has boosted the search for corresponding compounds. Minerals have always been a source of inspiration for the design of new materials. Among them, the pyroxenes, a major class of minerals that constitutes more than 20 volume% of the Earth's crust, have a flexible, quasi-one dimensional architecture with all the necessary ingredients to achieve the complex magnetic structures required for multiferroicity.

In recent years, the coupling between magnetic and electric properties in transition metal oxides has given rise to a significant research effort. This effort is driven by the emergence of new fundamental physics and potential technological applications, for instance in memories and logic devices. In 2009, Khomskii proposed a classification of multiferroics into two categories. For Type-I multiferroics, the ferroelectric order does not depend on the magnetism. Contrarily, in Type-II multiferroics, the ferroelectricity is actually induced by the appearance of magnetic order. As an obvious consequence, a large magneto-electric coupling can be achieved in the Type II case.

However, the microscopic mechanism governing the induction of ferroelectricity by the spin ordering is not yet fully understood and various mechanisms have been proposed, depending on the compound. In all cases, the appearance of ferroelectric polarization can be considered as a side effect of the symmetry-breaking caused by the magnetic ordering. So, one way to design new type II multiferroics is to induce complex magnetic orders that lead to a low symmetry, and especially polar symmetry. In recent years, two ingredients have proved to be favourable for stabilization of such magnetic structures: magnetic "frustration" and low-dimensionality.

Pyroxenes are so-called chain-silicates of general composition $AMSi_2O_6$, where A stands for mono- or divalent metals while M represents divalent or trivalent metals. Their crystal structures having orthorhombic or monoclinic symmetries can accommodate a wide variety of M and A elements, especially the magnetic 3d-transition metals. In most cases, by appropriate synthetic routes, silicon may also be replaced by germanium. The pyroxene crystal structure presents isolated zig-zag chains of edge-sharing MO_6 octahedra giving rise to low-dimensional magnetic behaviour. These quasi-1D chains are bridged together by corner-linked SiO_4 tetrahedra chains and the general magnetic chain arrangement forms a triangular lattice which may result in magnetic frustration (three magnetic moments on a triangle cannot be simultaneously anti-parallel to each other). Thus, the pyroxenes are promising materials in the search for new multiferroics.

Since pyroxenes are known for the sensitivity of their properties to steric effects (that is, the size of the constituent atoms), we investigated synthetic pyroxene compounds with the heavy atom Strontium replacing the usual Calcium atom on the A site. We have synthesized powders and single crystals of $SrMGe_2O_6$ (with M = Cobalt or Manganese) and investigated in detail, for the first time, their crystal and magnetic structures, using both X-ray diffraction and neutron diffraction. We found that the compound $SrMnGe_2O_6$ indeed orders antiferromagnetically below a Néel temperature T_N = 4.5 K. Its magnetic structure is characterized by a cycloidal spin configuration (see Fig. 1). Such a structure can lead to ferroelectric order through the so-called Inverse Dzyaloshinskii-Moriya effect.

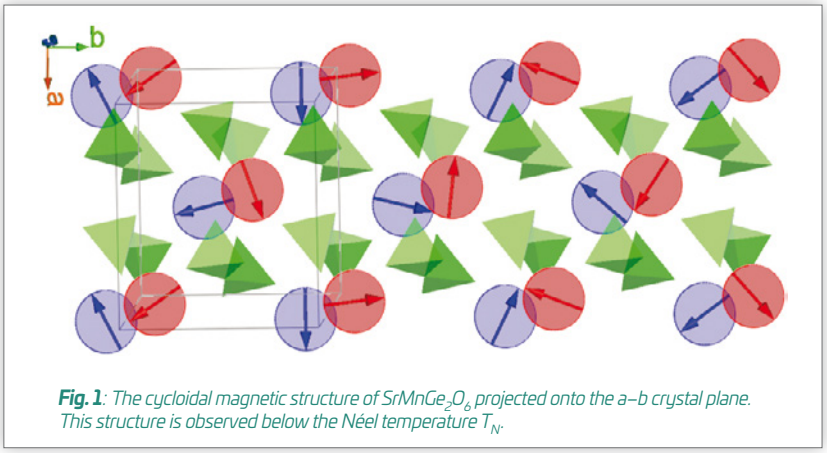

***Fig. 1**: The cycloidal magnetic structure of $SrMnGe_2O_6$ projected onto the a–b crystal plane. This structure is observed below the Néel temperature T_N.*

Measurements of the electrical properties (Fig. 2) show a spontaneous electric polarization developing precisely in coincidence with the magnetic ordering, proving that $SrMnGe_2O_6$ is indeed a new type II multiferroic, where the ferroelectricity is induced by a cycloidal spin structure. A large single crystal grown at the Institut NÉEL by Pascal Lejay is now being used for investigating the structural details of the magnetoelectric coupling, by diffraction and magnetic measurements.

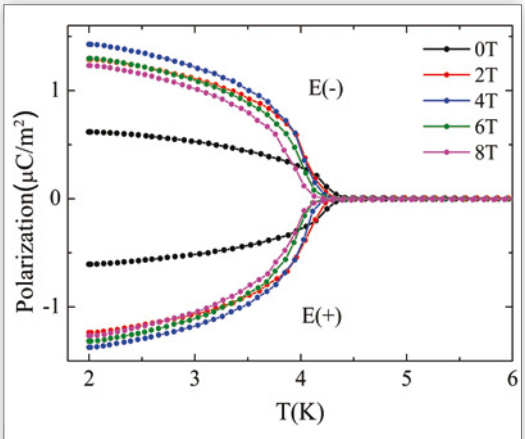

***Fig. 2**: The electric polarization induced by the magnetic order in $SrMnGe_2O_6$ below T_N = 4.5 K.*

CONTACT

Claire V. COLIN
claire.colin@neel.cnrs.fr

Céline DARIE
celine.darie@neel.cnrs.fr

Pierre BORDET
pierre.bordet@neel.cnrs.fr

PhD student:
Lei DING

FURTHER READING...

"$SrMGe_2O_6$ (M = Mn, Co): a family of pyroxene compounds displaying multiferroicity"
L. Ding, C. V. Colin, C. Darie and P. Bordet
***J. Mater. Chem. C* 4**, 4236 (2016).

"One-dimensional short-range magnetic correlations in the magnetoelectric pyroxene $CaMnGe_2O_6$"
L. Ding, C. V. Colin, C. Darie, J. Robert, F. Gay and P. Bordet
***Phys. Rev. B* 93**, 064423 (2016).

Influence of lattice vibrations on a quantum phase transition

In the vicinity of the absolute zero of temperature, all materials, except Helium, are solid. Analogous to this, the conduction electrons in certain metallic compounds can "freeze" at low temperature into a Charge-Density Wave phase: a stationary, ordered, spatial modulation of the electron density. If the temperature is raised, the charge density wave order is destroyed (it "melts"). This is a result of thermal fluctuations, as in a classical solid-to-liquid phase transition. But at zero temperature, in spite of the absence of any thermal fluctuations, it is possible to cause the charge density wave to melt due to quantum fluctuations. Such a transition is called a quantum phase-transition. To understand the rich physics associated with this type of transition, we need to know what drives the transition.

Charge density waves (CDW's) are a particularly interesting case where the electronic phase (*i.e.* the electron-density modulation) is associated with a lattice distortion. In order to decrease the electronic energy and due to a strong interaction between the conduction electrons and the lattice, the charge density wave alters the equilibrium position of the atoms, creating a periodic lattice distortion whose repeat-length is of the order of several lattice constants.

The atoms in a solid vibrate around their equilibrium positions. The oscillation amplitude is greater the higher the temperature, but even at zero temperature the vibration amplitude is non-zero. This is the "zero-point motion", a direct consequence of the Heisenberg uncertainty principle. The potential in which lattice atoms vibrate is usually approximated by a harmonic potential, i.e. an atom's potential energy is a quadratic function of its distance from its equilibrium position. In reality, this potential is not harmonic, which explains macroscopic physical properties of materials at high temperature such as thermal expansion. But this anharmonicity can have important consequences, even at zero Kelvin, for the stability of an electronic phase coupled to the lattice.

We have studied the spectrum of the lattice vibrations (the phonon spectrum) for the chalcogenide compound Niobium Diselenide ($NbSe_2$). This compound develops a charge density wave phase below temperature 33.5 K, and also superconductivity below 7.2 K (see Fig. 1). Our experiments were done on a dedicated X-Ray beamline (ID28) at the European Synchrotron Radiation Facility, Grenoble. We measured the loss of energy of the X-ray beam, scattered by the phonons in a 100 micron size sample of $NbSe_2$. The sample was placed in a sealed capsule of Helium compressed by two diamonds, situated in a cryostat. To tune $NbSe_2$ across its quantum phase transition, we applied hydrostatic pressures up to 40 000 atmospheres (4 GPascals), at various temperatures (see Fig. 1).

We observed that the energy of a specific phonon mode, the precursor of the lattice distortion, decreases as we lower the temperature towards the phase-transition – the phonon "softens". This is because, unlike in the case of a harmonic oscillator, the oscillation frequency (or the energy of the phonon) depends on the amplitude of the oscillation, which decreases with decreasing temperature. It is this weakening of the vibrations that triggers the freezing into the CDW phase at 33.5 K for P =0 (Fig. 1). Under pressure, the amplitude of the oscillation decreases and, intuitively, we expect that the atoms experience mainly the harmonic part of the potential. However, we observe that this same phonon softens significantly even at pressures above the critical pressure.

To account for the experimental results, the phonon spectra, including the effects of anharmonicity, were calculated from first principles by our colleagues at the Pierre & Marie Curie University, Paris (UPMC). Their calculations explain the experimental results both qualitatively and quantitatively over a wide range of temperature and pressure. They show that, in the CDW phase, the lattice potential for the atomic vibrations has a "double-well" shape. Each atom is "frozen" into one of the two wells, see sketch (i) in Fig. 1 which shows the CDW-related lattice distortion.

Squeezing the crystal lattice by applying pressure smoothes out the double well (sketches ii and iii), but this shape persists over a certain pressure range outside the charge density phase. So why has the lattice distortion disappeared in that range? The reason is that, even at low temperature, the atoms feel both wells due to their large zero-point motion.

Thus, the quantum vibration of the lattice atoms is the mechanism that drives the "melting" of the charge density waves at the quantum phase transition. We note finally that, as seen in Fig. 1, the superconductivity is only marginally affected by the presence of the charge density waves.

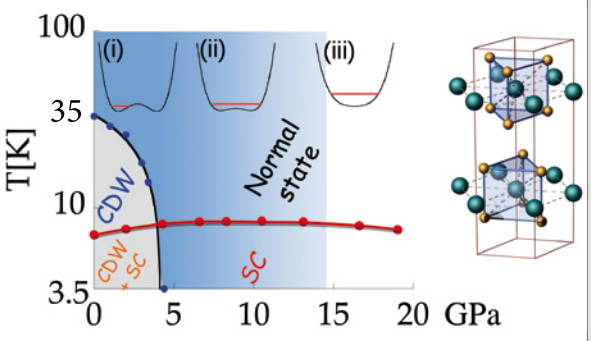

***Fig. 1 - At left**: P-T phase diagram for $NbSe_2$. Charge Density Waves are observed In the grey zone, coexisting with superconductivity (SC) below the red boundary. At 0 K, the charge density wave is stable up to 4.6 GPa pressure.*

***i, ii, iii**: Sketches of the potential energy of a lattice atom vs. its position, at T near 0 K, for three values of pressure. The red lines indicate the energy and the range of quantum motion of the atom. These atomic vibrations correspond to the specific phonon mode measured by X-Ray scattering.*

***At right**: Crystal structure of $NbSe_2$, a hexagonal lattice of Nb atoms (blue) sandwiched between surrounding Se atoms (gold).*

CONTACT

Pierre RODIÈRE
pierre.rodiere@neel.cnrs.fr

PhD student:
Maxime LEROUX

FURTHER READING...

"Strong anharmonicity induces quantum melting of charge density wave in 2H-$NbSe_2$ under pressure"
M. Leroux, I. Errea, M. Le Tacon, S. M. Souliou, G. Garbarino, L. Cario, A. Bosak, F. Mauri, M. Calandra and P. Rodière
***Phys. Rev. B* 92**, 140303(R) (2015).

"Anharmonic suppression of charge density waves in 2H-NbS_2"
M. Leroux *et al.*
***Phys. Rev. B* 86**, 155125 (2012).

NIKA2: revolutionary camera for millimetre waves sees first light

An important fraction of the matter in the universe is very cold, and emits only far infrared, microwave or millimetre wave radiation. To detect cold astronomical objects, a radiotelescope's detection instrument must be cooled to even lower temperatures, to avoid the thermal noise of the detector. NIKA 2, the second generation Neel-IRAM-KID-Array, is a dual-band millimetre-wave camera operating simultaneously at 150 and 260 GHz. The instrument is based on large arrays of superconducting Kinetic Inductance Detectors (KIDs) operated at temperature 0.1 Kelvin. NIKA 2 was built by an international consortium, led by the Institut NÉEL. Successful installation took place in October 2015 at the 30 m diameter telescope of the IRAM (Institut de Radioastronomie Millimétique) on Pico Veleta at altitude 2850 m in the Sierra Nevada, Spain.

NIKA 2's field of view has a diameter of 6.5 arcmin (0.1 degrees), with angular resolutions of 12 and 18 arcsec (3 and 5 millidegrees), at 1.15 and 2 mm wavelengths (260 and 150 GHz) respectively.

It is designed as a facility instrument (open to the astronomy community via competitive calls) that will remain at its present position for at least a decade.

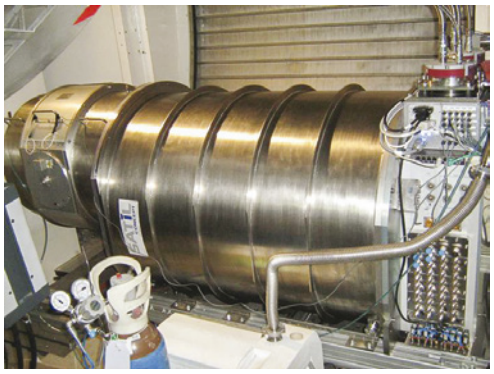

***Fig. 1**: The NIKA 2 dilution cryostat (about 1 m diameter, base temperature 100 mK), which was designed and fabricated at the Institut NÉEL, is shown mounted in the receiver cabin of the 30 m Pico Veleta Radio telescope.*

NIKA2 will address a vast range of scientific topics. For example, it will serve for studies of the intensity and polarization of the thermal emission coming from dust in galactic star-forming regions, and for observations of dust-obscured, optically-faint galaxies during their major episodes of formation in the very early universe. Over the next four years, the NIKA2 instrument consortium will carry out five, large, dedicated programmes during 1300 hours of guaranteed observation time on the Pico Veleta telescope.

The first testing and characterization of NIKA 2 took place only two weeks after installation, and showed

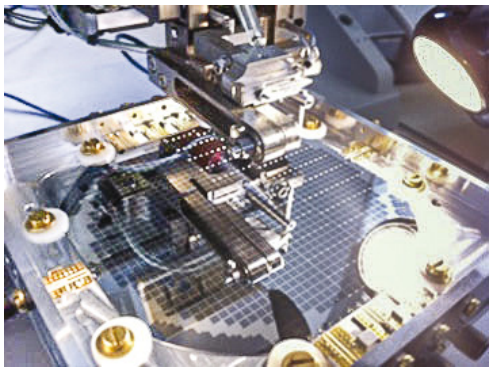

***Fig. 2**: One of the NIKA 2 camera's arrays being prepared at the Institut NÉEL's bonding machine. Each tiny square on the 80 cm diameter circular substrate is a millimetre-wave detector (a KID).*

that 80% of the KIDs were working as planned, with sensitivities in line with the original specifications and our in-lab tests. The readout electronics installed in January 2016 allowed simultaneous readout from the 3300 installed detectors. Further upgrades and in-depth characterization of the instrument are being done through 2016.

To give an idea of the sensitivity achieved, we have calculated that NIKA 2 could easily detect, from its current location in southern Spain, the thermal emission of one of the rabbits that populate the Institut NÉEL's car park in Grenoble, more than a thousand km away.

Access will be opened to international astronomers during the winter semester 2016/2017. To illustrate the system's performance, we show here (Fig. 3) a "first light" image obtained on the object DR21OH, a well-known star-forming region inside the Cygnus X molecular cloud complex.

***Fig. 3**: NIKA 2 maps of the DR21OH star-forming region at 260 GHz (left) and 150 GHz (right). The detected emission is mostly coming from cold interstellar dust, and would appear as a dark "string" at visible wavelengths. The maps are 13 arcmin (0.2 degrees) wide, the angular resolution in each band is represented as a white disk at the bottom left of the images.*

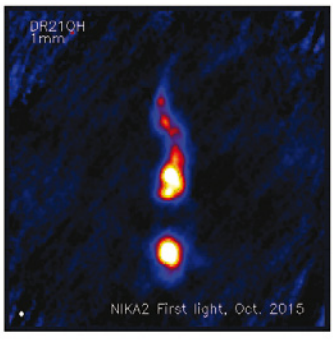

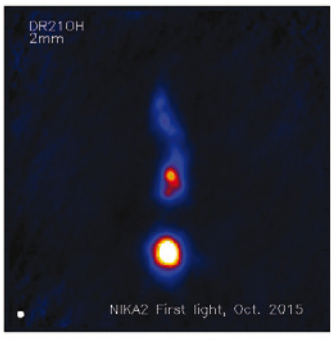

CONTACT

Alessandro MONFARDINI
alessandro.monfardini
@neel.cnrs.fr

FURTHER READING...

"The NIKA2 instrument, a dual-band kilopixel KID array for millimetric astronomy"

M. Calvo, A. Benôit, A. Catalano, J. Goupy, A. Monfardini, N. Ponthieu, E. Barria, G. Bres, M. Grollier, G. Garde, J.-P. Leggeri, G. Pont, S. Triqueneaux, and 35 national & international authors

***J. Low Temp. Phys* 184,** 816 (2016).

See also:
CNRS Press release

http://www2.cnrs.fr/presse/communique/4401.htm

Micro-transfer setup for assembling smart stacks

Recent, innovatory 2-Dimensional materials, such as graphene (a monolayer of carbon atoms) or transition metal di-chalcogenides (MoS_2, WSe_2...), can be assembled into a variety of heterostructures. These so-called "van der Waals" structures are opening up new fields for exploratory physics and applications. At the Institut NÉEL, we have developed a micro-transfer platform with a lateral mechanical-alignment precision of order one micron, which we use for making stacks of different 2D exfoliated materials.

A van der Waals heterostructure is a pile of lamellar materials where the successive layers are bound together by physical interactions (van der Waals forces) rather than by chemical bonds. The source lamellar materials are usually obtained by exfoliation of a crystal, a technique that gives single-monolayer flakes of very high crystalline quality. But these flakes are only a few tens of microns in width. Aligning a tiny sub-nm thickness flake precisely above another one, and then bringing them into perfect contact is a real challenge.

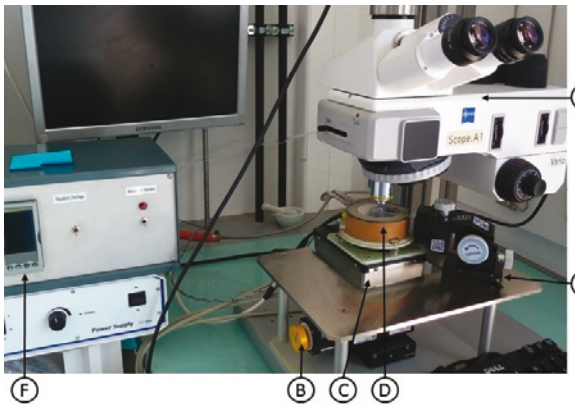

***Fig. 1 (a)**: The micro-transfer apparatus: the microscope and display, the XYZ displacement elements, the sample-holder component and temperature controller.*

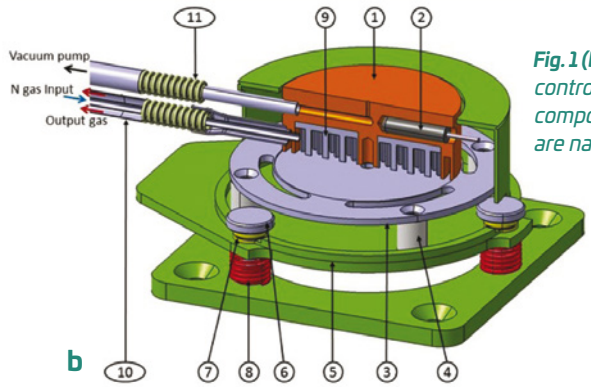

***Fig. 1 (b)**: The temperature-controlled sample-holder component. Items A-F and 1-11 are named in the text.*

Our method for assembling a pile of 3 to 10 monolayers on a substrate uses a transparent stamp to pick up, transport and deposit the layers one by one. The "stamp" is a glass slide with a spot of transparent, sticky, polymer film of PPC (polypropylene carbonate) on the under side.

Our micro-transfer platform (Fig. 1) is placed under a Zeiss Axio optical and digital microscope (A in Fig. 1a). A base-plate supports a motorized, high precision XYZ positioning system. This consists of two perpendicular horizontal motors (B) with 25 mm range, and a stepper-motorized elevator stage (C) that supports the substrate-holder part (D), providing the very precise vertical approach (200 nm steps) required during a transfer. Above the base-plate, a nickel-plated steel plateau carries a second, independent, hand-operated XYZ micro-positioner (E) (which has a magnetic base for initial placement). This positioner has a clamp to hold the glass microscope slide used to transport the flakes.

The substrate-holder part (see Fig. 1b) is fixed on the lower elevator stage. The heart of the device, the substrate holder itself, is a 2 inch diameter heating plate (>200° C) in nickel-plated copper (1 in Fig. 1b). The substrate is held over a 1 mm hole in the copper plate by aspiration (11). Thus no glueing is needed, so the plate's surface always stays clean.

The copper plate incorporates a Type J thermocouple (2) and is heated uniformly by two 175 W heating cartridges. It is supported by a stainless steel plate (3) mounted via insulating fibreglass pedestals (4) on a fibreglass screening plate (5). This has three adjusting screws (6) with spherical bearing surfaces (7), providing an angular adjustment ± 2° with respect to the XY plane, for bringing the substrate and the glass slide exactly parallel. Rapid cooling of the copper plate after a transfer operation is provided by a nitrogen gas circulation, fed via a flexible coaxial metal tube (10), through a dissipator chamber (9) inside the plate. A high precision PID (proportional-integral-derivative) temperature regulator with a Triac (electronic) output (F in Fig. 1a) stabilizes the copper plate within ±0.1 °C, essential for accurate control of the substrate temperature during the transfer.

The transfer procedure is as follows: After a lateral alignment to position the flake held on the stamp precisely above the flake on the substrate, the delicate step is contacting these two monolayer flakes together. A careful vertical displacement of the substrate enables us to see an initial zone of contact form between the substrate and the relatively thick and uneven polymer-film, at a random x,y location which can be quite far from the tiny flakes. The next, crucial step is achieved by moderate heating, which softens the polymer and enlarges the zone of contact to include the zone of interest, at a speed that depends on the speed of the temperature ramp. This provides a smooth landing for the upper flake, which binds atomically onto its target. The ultimate step is heating up to 120 °C: The polymer melts and liberates the transported monolayer flake.

Our substrate-holder unit is open to wide possibilities such as integration in a glove box, to limit oxidation and pollution of the layers. Also, the platform can precisely align mechanical masks and place single monolayers over pierced holes in a substrate, for their strain-free suspension.

***Fig. 2**: Optical image of a BN/Graphene/BN tri-layer realized with this system (A. Jordan, B. Sacépé). The top Boron Nitride monolayer-flake appears in pale yellow, the bottom BN flake in blue. (The graphene layer is invisible between them.)*

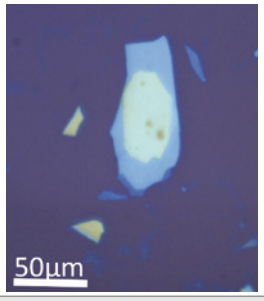

CONTACT

Didier DUFEU
didier.dufeu@neel.cnrs.fr

Laëtitia MARTY
laetitia.marty@neel.cnrs.fr

Benjamin SACÉPÉ
benjamin.sacepe@neel.cnrs.fr

PhD student:
Goutham NAYAK
Katrin ZIMMERMANN

Fragmentation of magnetism

In physics as in chemistry, it is well known that matter can become ordered, as for example in a crystalline solid, when cooled to sufficiently low temperature. There also exist systems that remain disordered in the manner of a gas or a liquid, even at the lowest temperatures accessible experimentally. What is much more rare, if ever observed, is a state of matter that would be both ordered and disordered everywhere in the system, *i.e.* that would be both solid and liquid for example.

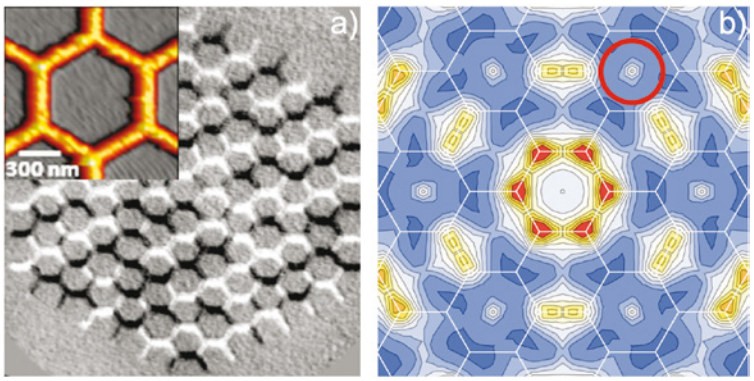

***Fig. 1**: **(a)** Magnetic image (10µm x 11µm) of a honeycomb array of ferrimagnetic-alloy nanomagnets with size approx. 500x100x10 nm³), obtained with a photoemission electron microscopy technique at the ELETTRA facility. The black and white contrast gives the local direction of the magnetization (pointing left or right) within each individual nanomagnet. nset (top left): Topographic image obtained with an Atomic Force Microscope.*

***(b)** Representation in reciprocal space of the magnetic phase reconstructed mathematically (a Fourier transform) from the real space image shown in (a). The diffuse background, associated with the magnetic disorder, appears in yellow. Six Bragg peaks (one of them indicated by a red circle) are also visible. The coexistence of this diffuse background and the Bragg peaks demonstrates the coexistence of magnetic order and disorder here, i.e. "fragmentation" of magnetism.*

Such a phase, simultaneously liquid and solid, can be observed in a magnetic "meta-material". We emphasize here that we are not considering a magnetic equivalent of a glass of water containing ice cubes, which would be, simply, a system presenting a coexistence of two phases, physically separated and out of thermodynamic equilibrium. Instead, what we mean is a magnetic equivalent of a glass of water that would be liquid and ice everywhere in the glass, at any time.

It is difficult to get a mental representation of such a system and it may be convenient to visualize it, not in real space, but in reciprocal space. Indeed, if we could achieve a diffraction pattern of such an exotic state of matter, we would observe two features simultaneously. This pattern would present very intense points in some specific regions of the reciprocal space, called Bragg peaks, associated with the existence of a periodic arrangement and reflecting the symmetry of the solid. But this diffraction pattern would also show a diffuse background signal, associated with the disorder present in the system. It is important to stress once more that these two characteristics of the diffraction pattern would be representative of a state of matter at thermodynamic equilibrium.

In a collaboration with the Nanospectroscopy beamline staff at the ELETTRA synchrotron radiation facility (Trieste), researchers of the Institut NÉEL and the Jean Lamour Institute (at Nancy) have fabricated a magnetic meta-material that exhibits all the characteristics of such an exotic state of matter. This magnetic meta-material is just an array of nanomagnet bars arranged on a lattice having a honeycomb-type hexagonal geometry. When the size of these nanomagnets is carefully chosen, their individual magnetization can be in two states, and in two states only, aligned left or right along the long axis of the bars. We can then shake the system of magnets (using a magnetic field or the temperature) to bring it into a magnetic state that minimizes its configurational energy.

When the state resulting from this process is imaged in real space, the magnetic configuration (the arrangement of left or right orientations of the individual magnets) seems, essentially, disordered. Looking at it more carefully, a trained eye could find some periodic, magnetic patterns (see Fig. 1a). Sometimes, but not everywhere ! This is why it is useful to visualize the resulting magnetic configuration in reciprocal space (Fig. 1b). When doing so, the corresponding "diffraction" pattern shows a coexistence of Bragg peaks and a diffuse background, thus indicating that the system is both ordered and disordered. The challenge is then to demonstrate that this is not a coexistence of two out-of-equilibrium phases, but a state of matter that is both liquid and solid, everywhere in the lattice, at thermodynamic equilibrium.

A detailed analysis of the magnetic configuration reveals that the system acts as if each individual nanomagnet of the lattice was split into two distinct components. For this reason, we say that the magnetism is "fragmented": an internal degree of freedom (the magnetization of the nanomagnets) is somehow cut into two pieces, resulting in a collective phase which is at the same time ordered and disordered, solid and liquid, at thermodynamic equilibrium.

This exotic state of matter is not specific to our artificial magnetic structures: we have also observed it in a bulk compound synthesized chemically. Achieving complete, fine tuning of this fragmentation of magnetism is now an ultimate goal. It would provide new opportunities to understand, realize and control new states of condensed matter, be they artificial or not.

CONTACT

Benjamin CANALS
benjamin.canals@neel.cnrs.fr

Nicolas ROUGEMAILLE
nicolas.rougemaille@neel.cnrs.fr

PhD student:
Ioan-Augustin CHIOAR

FURTHER READING...

"Fragmentation of magnetism in artificial kagome dipolar spin ice"
B. Canals, I.-A. Chioar, V.-D. Nguyen, M. Hehn, D. Lacour, F. Montaigne, A. Locatelli, T. O. Mentes, B. Santos Burgos, N. Rougemaille
***Nat. Commun.* 7**, 11446 (2016).

"Observation of magnetic fragmentation in spin ice"
S. Petit, E. Lhotel, B. Canals, M. Ciomaga Hatnean. J. Ollivier, H. Mutka, E. Ressouche, A. R. Wildes, M. R. Lees, G. Balakrishnan
***Nat. Phys.* 12**, 746 (2016).

Tracking the composition of carbon-black samples from Pompeii

A better knowledge of past societies and of their degree of technological development can come from scientific analysis of archaeological remains. However, the study of residues from archaeological finds poses a series of challenges for materials science. Carbon-based materials, easy to make by burning diverse organic matter, have been used since prehistoric times as pigments for drawings and paintings and also as dyes, inks and cosmetics. These materials are often ill-ordered and it has not been easy to characterize their specificities and their differences by traditional crystallography. Now, the identification, quantification and mapping of the different phases in such heterogeneous samples can be accomplished using synchrotron based techniques.

The excellent preservation state of the Pompeii ruins and of many everyday objects, since the eruption of Mount Vesuvius in AD 79, represents an extraordinary opportunity for studying Roman society. In our work, black powders found in Pompeii houses in different types of closed containers were characterized in order to assess a correspondence between the composition and the type of container and to specify the use of these compounds as ink and/or cosmetics.

We have investigated five micro samples from the Roman carbon black found in Pompeii and preserved in their original containers made of glass or bronze (Fig. 1). Preliminary studies of these precious materials in the laboratory revealed their complexity: they contain both amorphous and crystalline constituents. For a precise analysis of these heterogeneous samples, we proposed a new methodology employing synchrotron radiation. The measurements were done at the French Collaborative Research Group's beamline (BM2-D2AM) at the European Synchrotron Radiation Facility, Grenoble.

We first identified and quantified the crystalline phases present by using a combination of X-ray powder diffraction and elemental microanalysis, assisted by Computed Tomography. This technique allows us to localize in 3D the different constituent phases in a sample and to extract their individual diffraction diagrams. Secondly, we used analysis of the Pair Distribution Function (*i.e.* the distribution of the inter-atomic distances), utilizing the entire Bragg diffraction and diffuse scattering signal from a sample, to obtain information about the non-crystalline (amorphous) phase. This was identified as non-graphitic carbon: planes of carbon with nearest and next-nearest carbon-carbon bond distances of 1.4 and 2.4 Angstroms respectively, as in a graphite-layer plane, but without ordering perpendicular to these planes. Data sets for reference samples were used as models for the amorphous phase to determine its content in each sample. In the last step, the pair distribution functions were modelled in order to determine the fractions of amorphous and crystalline phases.

Thanks to this procedure, a description of the entire content of this kind of archaeological sample could be achieved for the first time. It allowed us to clarify the composition of the mixtures contained in three different types of containers. The origin of the carbon black pigments was obtained: We were able to demonstrate the use of charred vegetable materials, independently of the shape and the nature of the container. This means that in Pompeii, at AD 79, carbon-based inks were still in use for writing, and metallic inks had not yet been introduced.

As concerns the crystalline fractions, three of the samples contain well-known mineral phases or metallic compounds resulting from degradation of the bronze container. The two other samples reveal unexpected mineral phases of calcium phosphate, namely whitlockite $Ca_9(Fe,Mg)(PO_3OH)(PO_4)_6$ and phosphohedyphane $Ca_2Pb_3(PO_4)_3Cl$. We now have to extend the archaeological corpus in order to study the occurrence of these two exotic minerals in other similar samples and to understand the conditions of their formation.

Very recently (P. Tack *et al.*, 2016), the presence of lead atoms was reported in the ink of two papyrus fragments from the nearby site of Herculaneum, contemporaries of our Pompeian containers. Although the precise state of this lead was not determined, the elemental composition of the unknown lead-containing ingredient appears compatible with that of the phosphohedyphane phase of the Pompeii pigments. Further investigations are underway to determine if this rare mineral phosphohedyphane can be used as a tracer of the origin of ancient Roman inks.

***Fig. 1**: **At left**, containers for ink and cosmetics from the excavations at Pompeii. **At right**, optical microscope image of an archaeological sample, showing the heterogeneous nature and the complexity of the powder, which consists of particles having widely varying shapes, sizes and compositions.*

CONTACT

Pauline MARTINETTO
pauline.martinetto@neel.cnrs.fr

Pierre BORDET
pierre.bordet@neel.cnrs.fr

FURTHER READING...

"Identifying and quantifying amorphous and crystalline content in complex powdered samples: application to archaeological carbon blacks"

S. Cersoy, P. Martinetto, P. Bordet, J. L. Hodeau, E. Van Elslande and P. Walter

***J. Appl. Cryst* 49**, 585-593 (2016).

New generation of white phosphors for LED lighting

Devices based on light emitting diodes (LEDs) are a major disruptive technology expected to dominate the lighting market in the near future. The advantages of solid-state lighting sources are their energy saving (more than 50% compared to conventional fluorescent lamps) and their potential to produce high stability, long lifetime devices. White light is obtained by combining blue light from the LED with yellow light from a phosphor powder, usually containing a lanthanide rare-earth element. At the Institut NÉEL, we are developing a new type of phosphor based on aluminum-borate powders, composed of non-toxic and abundant elements, and especially without using any lanthanide.

The innovative feature of our phosphors is to produce a broad luminescence band throughout the visible spectrum yielding comfortable and safe lighting. The dominant system (around 98% of the market) for producing commercial white-light emitting diodes is based on an Indium Gallium Nitride (InGaN) chip emitting blue light, which is partially converted to yellow by a Cerium-doped Yttrium Aluminium Garnet (Ce^{3+}:YAG) phosphor placed just above the LED. However, due to the lack of a red light component, these phosphors produce bluish white emissions with low values of their "Colour Rendering Index" (the industry standard that effectively compares their colour to black-body light). This yields optically-uncomfortable light-sources, associated with blue-light hazards such as possible retinal damage and disturbance of the biological clock.

To avoid these serious disadvantages, a very large research effort is being undertaken to develop new combinations consisting of LEDs emitting in the blue or near-ultraviolet with new phosphors to produce a comfortable and safe warm-white light, *i.e.* containing a sufficient orange-red component. Moreover, the use of lanthanides in the phosphors should be avoided: Reducing the use of lanthanides is crucial because of the strong increase in prices since 2011, a consequence of the near-monopoly held by China on these elements strategic in the field of materials for energy.

The phosphors we are developing are based on Yttrium Aluminium Borate powders, without any added lanthanide ions. They are composed of non-toxic and abundant elements which make them inexpensive. The powders are prepared from solutions. Evaporation of the solvents leads to a viscous resin which then undergoes different thermal treatments under controlled atmospheres leading to beige-coloured powders.

The innovative property of these phosphors is their broad and intense photoluminescence extending over the whole visible range, 400-800 nm, under excitation with UV light (see Fig. 1). The origin of this intense emission is structural defects or organic radicals formed during the thermal treatment within the amorphous matrix. Thus, using only a single phosphor material, we can generate white light from an initial LED that emits in the near ultra-violet.

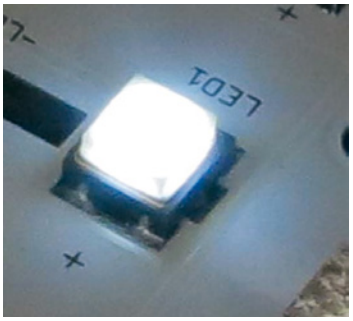

***Fig. 2**: A first prototype lighting device involving a UV-LED exciting an Yttrium Aluminium Borate phosphor powder dispersed in a silicone matrix.*

In fact, the main objective of our work is to understand the origin of the light-emitting centres, which are related to structural defects or organic radicals. For that, different spectroscopies and structural-study methods coupled with thermal analyses are implemented. Thus, the optimization of the chemical compositions, the synthesis procedures and the thermal treatments should increase the number of luminescent centres to enhance the luminescence properties. Another crucial point is to increase the absorption of the excitation light to improve the overall photoluminescence efficiency. Based on these promising properties, we have developed a prototype device (Fig. 2) to estimate the lighting performance of this new family of phosphors.

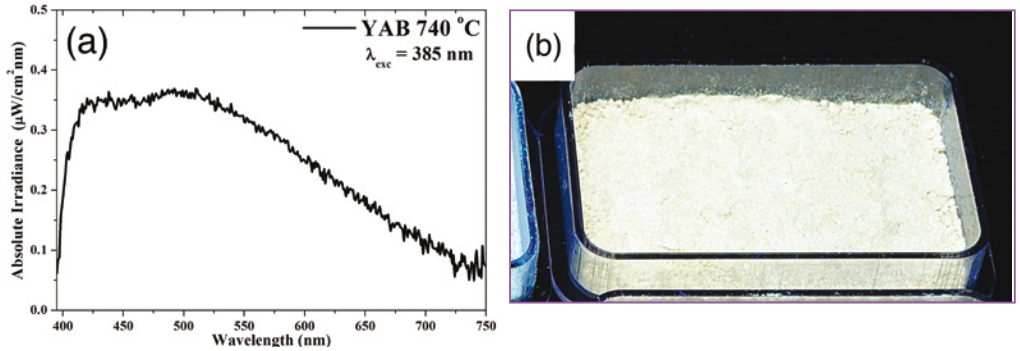

***Fig. 1 (a)**: Photoluminescence spectrum recorded for an Yttrium Aluminium Borate (YAB) powder calcinated at 740 °C. The emission is excited by an ultraviolet LED (wavelength 385nm). **(b)** Luminescent YAB powder under UV light.*

CONTACT

Alain IBANEZ
alain.ibanez@neel.cnrs.fr

Isabelle GAUTIER-LUNEAU
isabelle.gautier-luneau
@neel.cnrs.fr

PhD students:
Vinicius GUIMARAES
Pauline BURNER

FURTHER READING...

"Toward a new generation of white phosphors for solid-state lighting using glassy yttrium aluminoborates"

V. F. Guimarães, L. J. Q. Maia, I. Gautier-Luneau, C. Bouchard, A. C. Hernandes, F. Thomas, A. Ferrier, B. Viana and A. Ibanez

***J. Mater. Chem. C* 3,** 5795-5802 (2015).

A quantum phase transition seen from 0 to 600 K

We are accustomed to attributing phase transitions from an ordered state towards a disordered state to a temperature increase that agitates the atoms till the order is totally broken at a critical temperature T_c. However, this type of transition can also occur at strictly zero absolute temperature, when a parameter such as pressure or magnetic field or (in the case of an alloy) the proportion x of one component is varied. The "agitation" is now furnished by quantum fluctuations originating from Heisenberg's Uncertainty Principle, which allows the system to explore beyond its stability region. Such a transition is called a quantum phase-transition and the transition point is called the quantum critical-point. Quantum phase transitions have been studied previously only in systems with low values of T_c (<30 K). In fact, surprisingly, the effects of a quantum critical point can be visible up to arbitrarily high temperature in certain systems.

An interesting material to study in this respect is the alloy of the elements chromium and rhenium ($Cr_{1-x}Re_x$). Pure chromium is antiferromagnetic (*i.e.* it has an antiparallel ordering of neighbour atoms' magnetic moments) up to a critical temperature (called in this case the Néel temperature T_N) of 311 K. With 5-10% of rhenium added, it is antiferromagnetic up to temperatures as high as 600 K.

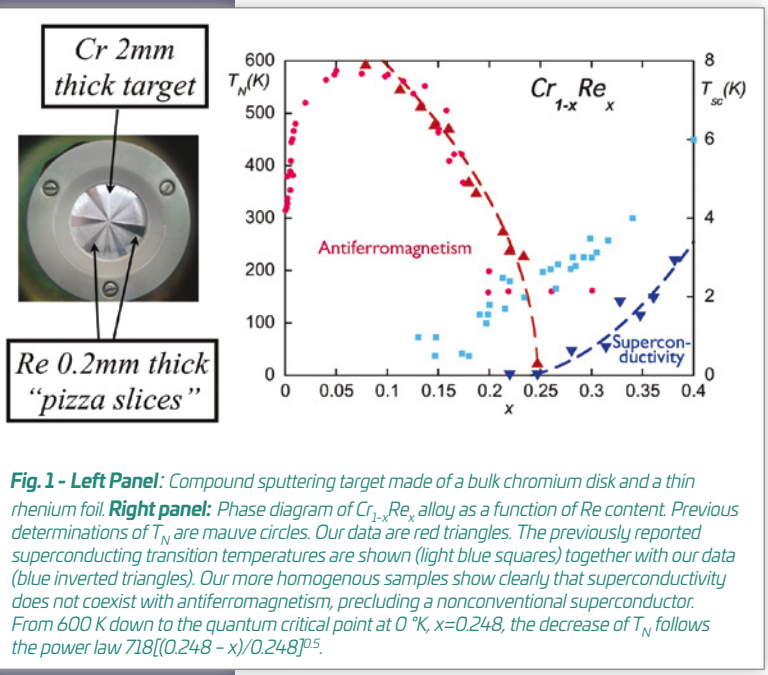

***Fig. 1 - Left Panel**: Compound sputtering target made of a bulk chromium disk and a thin rhenium foil. **Right panel:** Phase diagram of $Cr_{1-x}Re_x$ alloy as a function of Re content. Previous determinations of T_N are mauve circles. Our data are red triangles. The previously reported superconducting transition temperatures are shown (light blue squares) together with our data (blue inverted triangles). Our more homogenous samples show clearly that superconductivity does not coexist with antiferromagnetism, precluding a nonconventional superconductor. From 600 K down to the quantum critical point at 0 °K, x=0.248, the decrease of T_N follows the power law $718[(0.248 - x)/0.248]^{0.5}$.*

Another interesting property of these materials was reported 30 years ago: At very low temperature they are superconducting for concentrations x near the value 0.25 where the antiferromagnetic order disappears. Superconductivity has often been observed around a quantum critical point, but its origin remains mysterious even if quantum fluctuations are suspected to some extent.

Unfortunately, chromium evaporates at the melting point of rhenium, making it very difficult to manufacture chromium-rhenium alloys with accurately defined compositions: They tend to be uncontrollably Rhenium rich. We have circumvented this obstacle by using a sputtering (*pulvérisation*) technique. A plasma having the desired proportions of Cr and Re is generated by sputtering a combined target (see Fig. 1, left), and the plasma constituents deposit onto a substrate. Annealing and high temperature electrical resistivity measurements were done simultaneously in a fast optical furnace developed at the Institut NÉEL. Low temperature measurements were done in ^{3}He and ^{4}He cryostats.

As concerns the low-temperature superconductivity, we found that – contrary to the old data obtained with less well controlled samples – superconductivity appears only in the rhenium-rich region beyond the quantum critical point at x_c= 0.25. So that property is due to the addition of rhenium to the cubic crystal structure, and not to quantum antiferromagnetic fluctuations from chromium as has been suspected in the past.

Our low temperature measurements established the precise position of the quantum critical point for this alloy to be at x_c= 0.25. We found that the Néel temperature increased continuously from this critical point up to the highest obtained value of T_N =600 K, see Fig. 1. (The anomalous, old data for 160 K, red points in Fig. 1, are again clearly due to the limited quality of the alloys available at that time.) As a function of the alloying parameter x, the parameter T_N followed a power law with a 1/2 exponent, *i.e.* T_N is proportional to $(x_c - x)^{1/2}$. This power law is a defining characteristic of a quantum phase transition. It undoubtedly means that the quantum critical point, i.e. quantum fluctuations, control the transition to the antiferromagnetic phase all the way from T= 0 K to T= 600 K, a very unexpected result .

We have compared this Cr-Re alloy system to other alloy systems in order to understand why this material is affected by the quantum critical point up to such unusually high temperatures. Systems with long coherence lengths have a more usual exponential dependence far from the QCP, and the 1/2 power law installs itself only near to this point, while systems with short coherence lengths show a quantum-controlled behaviour at all temperatures.

Using the known dependences for T_c and coherence lengths, we have determined a general criterion for the crossover, as a function of an external parameter such as concentration, from the region controlled solely by thermal fluctuations to the region where quantum effects become observable. It shows that the properties of materials with low coherence lengths will be altered far away from the quantum critical points, up to unexpected high temperatures.

CONTACT

Manuel NÚÑEZ-REGUEIRO
nunez@neel.cnrs.fr

FURTHER READING...

"Experimental consequences of quantum critical points at high temperatures"
D. C. Freitas, P. Rodière, M. Núñez, G. Garbarino, A. Sulpice, J. Marcus, F. Gay, M. A. Continentino and M. Núñez-Regueiro
***Phys. Rev. B* 92**, 205123 (2015).

10TH ANNIVERSARY

HIGHLIGHTS 2016

Institut NÉEL

25, rue des Martyrs | BP 166
38042 Grenoble cedex 9 | France

neel.cnrs.fr

UNIVERSITÉ Grenoble Alpes

cnrs